Journal of Paleontology, 97(6), 2023, p. 1309–1328

0022-3360/23/1937-2337
doi: 10.1017/jpa.2023.80

JOURNAL OF PALEONTOLOGY
A PUBLICATION OF THE Paleontological SOCIETY

Echericetus novellus n. gen. n. sp. (Cetacea, Mysticeti, Eomysticetidae), an Oligocene baleen whale from Baja California Sur, Mexico

Atzcalli Ehécatl Hernández-Cisneros,[1]* Tobias Schwennicke,[2] Heriberto Rochín-Bañaga,[3] and Cheng-Hsiu Tsai[4]*

[1]Instituto Politécnico Nacional – Centro Interdisciplinario de Ciencias Marinas, Av. Instituto Politécnico Nacional, Playa Palo de Santa Rita, Postal mail 592, ZIP 23096, La Paz, Baja California Sur, México <atz_nemesis@hotmail.com>
[2]Departamento Académico de Ciencias de la Tierra, Universidad Autónoma de Baja California Sur, Carretera al Sur Km 5.5, Postal mail 19-B, ZIP 23080, La Paz, Baja California Sur, México <tobias@uabcs.mx>
[3]Department of Earth Sciences, University of Toronto, 22 Russell Street, Toronto, Ontario M5S 3B1, Canada <heriberto.rochinbanaga@mail.utoronto.ca>
[4]Department of Life Science and Institute of Ecology and Evolutionary Biology, National Taiwan University, No. 1, Sec. 4, Roosevelt Rd., Taipei, 106-17, Taiwan <whaletsai@ntu.edu.tw; craniata@gmail.com>

Non-technical Summary.—The name eomysticetids refers to the "dawn" of the baleen whale, suggesting the critical role in understanding the origin and early evolution of baleen whales. Eomysticetids represent an early diverging lineage showing the baleen-assisted feeding mode—an essential feature for baleen whales, including giant animals such as the blue or fin whales. This paper describes a new eomysticetid species—*Echericetus novellus*—from the Oligocene of Mexico, about 28 million years old. Our discovery of a new species of Oligocene eomysticetids from Mexico shows a much broader global distribution and higher diversity than previously recognized. The existence of *Echericetus novellus* from Mexico indicates that eomysticetids also inhabited warmer waters in the Northern Hemisphere instead of primarily higher latitudinal regions. Last, our discovery of a new but extinct eomysticetid from the Oligocene of Mexico provides new insights into the distribution pattern and habitat use of Eomysticetidae, which helps to decipher the ultimate demise of this once-successful baleen whale lineage.

Abstract.—Among the several evolutionary lineages of the baleen whales (Mysticeti), the eomysticetids are an ancient successful family that retain possibly nonfunctional teeth and functional baleen, a transitional stage between toothed and baleen-assisted filter-feeding mysticetes. The patchy fossil record leaves gaps in eomysticetid paleobiology interpretations, but their diversity and widespread geographical distribution can be a relevant proxy to understanding the evolution of crown Mysticeti. Here we describe a new baleen whale, *Echericetus novellus* n. gen. n. sp., from the Oligocene of Mexico (slightly older than 27.95 million years ago). This new taxon has morphological features that show its affinity to Eomysticetidae, such as the intertemporal region longer than wide, the elongate and oval temporal fossa, and a well-developed and lobate coronoid process of the mandible. Similarly, our cladistic analyses confirm the inclusion of *Echericetus* in the Eomysticetidae. *Echericetus* reinforces our notion of the eomysticetid diversity and disparity. Geographically, the existence of *Echericetus* from Mexico also indicates that eomysticetid inhabited subtropical regions in the Northern Hemisphere. Last, our discovery of a new eomysticetid from the Oligocene of Mexico provides new insights into the distribution patterns and habitat use of Eomysticetidae, essential to further explain the demise of this transitional lineage between toothed and baleen-bearing whales.

UUID: http://zoobank.org/00cfc802-e2da-465c-9bb6-59347be00164

Introduction

The Oligocene, ranging approximately from 34 to 23 Ma, witnessed an unparalleled period for the early evolution and diversification of Mysticeti, the largest mammals ever to have evolved (Marx and Fordyce, 2015; Tsai and Kohno, 2016). Groups such as eomysticetid are examples of great diversity and disparity, where developmental processes (Boessenecker and Fordyce, 2015b) and environmental factors (e.g., climate change; Marx et al., 2019) likely drove their evolutionary pathways. Eomysticetid display a widespread geographic distribution, unique long-irostrine skull morphology, and possible ecological role as a planktivore (Sanders and Barnes, 2002b; Clementz et al., 2014; Boessenecker and Fordyce, 2015b, 2017b). More interestingly, eomysticetid represent a transitional step between the

*Corresponding author.

toothed and baleen-bearing mysticetes despite no fossil evidence of baleen in Oligocene mysticetes yet (Boessenecker and Fordyce, 2015b; Marx et al., 2017; Gatesy et al., 2022). The eomysticetid fossil record is primarily in the South Pacific Ocean (New Zealand). However, the Northern Hemisphere has also produced abundant eomysticetid fossils (Sanders and Barnes, 2002a, b; Peredo and Uhen, 2016; Peredo et al., 2018; Hernández-Cisneros and Nava-Sanchez, 2022).

Here we describe a new eomysticetid genus and species (Mysticeti, Eomysticetidae) from the Oligocene of Mexico (La Paz, Baja California Sur; Fig. 1). The holotype of this new taxon, MRAHBCS Pal/V119, was excavated and collected in 1995 (Schwennicke et al., 1996). Previously, this specimen was tentatively considered similar to "*Mauicetus*" *lophocephalus* (Barnes, 1998), now known as the eomysticetid *Tokarahia lophocephalus* (Boessenecker and Fordyce, 2015a). In addition to the anatomical description, we analyze its phylogenetic relationships within Cetacea and interpret eomysticetid morphological disparity and diversification.

Geological setting

The specimen MRAHBCS Pal/V119 (*Echericetus novellus* n. gen. n. sp.), recovered in 1995, was found in a marine bed poorly exposed at the bottom of an ~5 m wide dry streambed. At this site, the fossil-bearing bed and the strata below were not exposed adequately (see Schwennicke et al., 1996). However, during visits to the locality area in 2018 and 2021, we observed that these strata are exposed about 30 m to the northeast of the original fossil site. Beds dip ~3° southwest, which explains why these beds have not been exposed at the position where *Echericetus novellus* n. gen. n. sp. has been found. For the present paper, we gathered new stratigraphic field data and obtained a radiometric age from a tuff bed; these data allow a more detailed stratigraphic interpretation.

The lowermost unit, named bed 0 by Schwennicke et al. (1996), is a large-scale cross-bedded fine-grained arkosic sandstone, seemingly of eolian origin. About 1 m is exposed. We consider this bed as part of the Upper Oligocene–lowermost Miocene Salto Formation exposed north and east of La Paz and elsewhere in Baja California Sur along its eastern margin (McFall, 1968; Hausback, 1984; Schwennicke et al., 2000, 2006; Umhoefer et al., 2001; Plata-Hernández, 2002; Alvarado-Gastelum, 2007; Drake et al., 2017). The distance from the fossil site (Bed 2; see Fig. 1) to the southernmost exposures of the Salto Formation east of La Paz (called Cerro Chichonal sandstone by Aranda-Gómez and Pérez-Venzor, 1988) is 18 km. The Salto Formation accumulated in terrestrial, coastal areas in alluvial fan and eolian settings. The unit is contemporaneous with the marine San Juan Member of the El Cien Formation (Fischer et al., 1995; Alvarado-Gastelum, 2007) exposed in San Juan de la Costa (late Early Oligocene, but also see Hernández-Cisneros and Nava-Sánchez, 2022, p. 3, fig. 3).

The Salto Formation is discordantly overlain at the fossil site by the marine beds, which contained the mysticete described herein (bed 2; see Fig. 1). The lowermost layer on the erosional surface is a sandy conglomerate (bed 1) that grades laterally into conglomeratic sandstone. The clasts are mainly rounded pebbles, cobbles, and a few boulders of varying composition, including volcanic, plutonic, and metamorphic rocks. The sandy matrix contains some phosphatic grains and exhibits internal lamination (Schwennicke et al., 1996). This bed represents a gravelly beach deposit and marks the beginning of a marine transgression (Schwennicke et al., 1996). Some cobbles exhibit imbrication, indicating breaking waves from the southwest, suggesting a northwest–southeast-oriented shoreline. The basal conglomeratic texture of bed 1 grades upward into sandstone, mudstone, and greenish tuffaceous mudstone with sandstone lenses (bed 2). These sediments exhibit mainly parallel lamination in addition to some lenticular and flaser bedding. Bioturbation is nearly absent. In addition, at the top of bed 2, we found a lenticular reworked tuff up to 15 cm in thickness that was not observed by Schwennicke et al. (1996). This tuff has been used for radiometric dating, as explained in the following. Bed 2 reflects a lagoonal depositional environment influenced by volcanic activity (Schwennicke et al., 1996). Field observations in 1995 revealed that besides the recovered specimen MRAHBCS Pal/V119, there were two more poorly preserved mysticete fossils in bed 2 (one of them is the specimen MRAHBCS Pal/V141, an eomysticetid fragmented skull and vertebrae). All these fossils showed the same orientation (east–west direction), perhaps due to wave action or currents, and it seems likely that these fossilized mysticetes indicate a stranding event in the coastal lagoon environment (Schwennicke et al., 1996). Bed 2 grades upward into gray, slightly tuffaceous volcaniclastic sandstone of bed 3 (about 30 m thick). Texturally, bed 3 varies from regularly sorted, silty fine-grained sandstone to poorly sorted, fine- to coarse-grained sandstone. The silty sandstone is found predominantly in the lowermost portion of bed 3. Some volcanic granules and pebbles are scattered in the rock or form thin conglomeratic lenses. Whereas the bottom 2 m of bed 3 commonly is finely laminated, the middle and upper parts of bed 3 also exhibits cross-bedding and cross-lamination. Volcanic influence during deposition of bed 3 is also revealed by a 20 cm thick bed of reworked fine-grained tuff not recognized by Schwennicke et al. (1996). Bed 3 reflects a distal fluvial depositional setting and grades upward into coarser muddy sandstone and pebbly sandstone (bed 4; Schwennicke et al., 1996, p. 4, fig. 3), all it of volcaniclastic composition (Fig. 1).

The sedimentology and stratigraphy of the succession at the fossil site suggest that beds 1 and 2 reflect a short-lived marine transgression in the area. To obtain more information related to the age of this event (and the age of the specimen of *Echericetus novellus* n. gen. n. sp. at the bottom of bed 2), we searched the marine sediments of beds 2 and 3 for micro- and nannofossils, but unfortunately none could be found. However, we dated the already mentioned reworked tuff at the top of bed 2. The U–Pb zircon age of this tuff is 27.95 ± 0.16 Ma (latest Rupelian, late Early Oligocene; Cohen et al., 2023). This age is similar to the age of the middle San Juan Member of the marine El Cien Formation at San Juan de la Costa (Schöllhorn et al., 2020). We therefore conclude that the marine beds 1 and 2 in the study area are contemporaneous with the middle part of the San Juan Member and may represent a marginal facies of this unit. The fluvial deposits of beds 3 and 4 (Schwennicke et al., 1996, p. 4, fig. 3) are therefore interpreted as basal strata

https://doi.org/10.1017/jpa.2023.80 Published online by Cambridge University Press

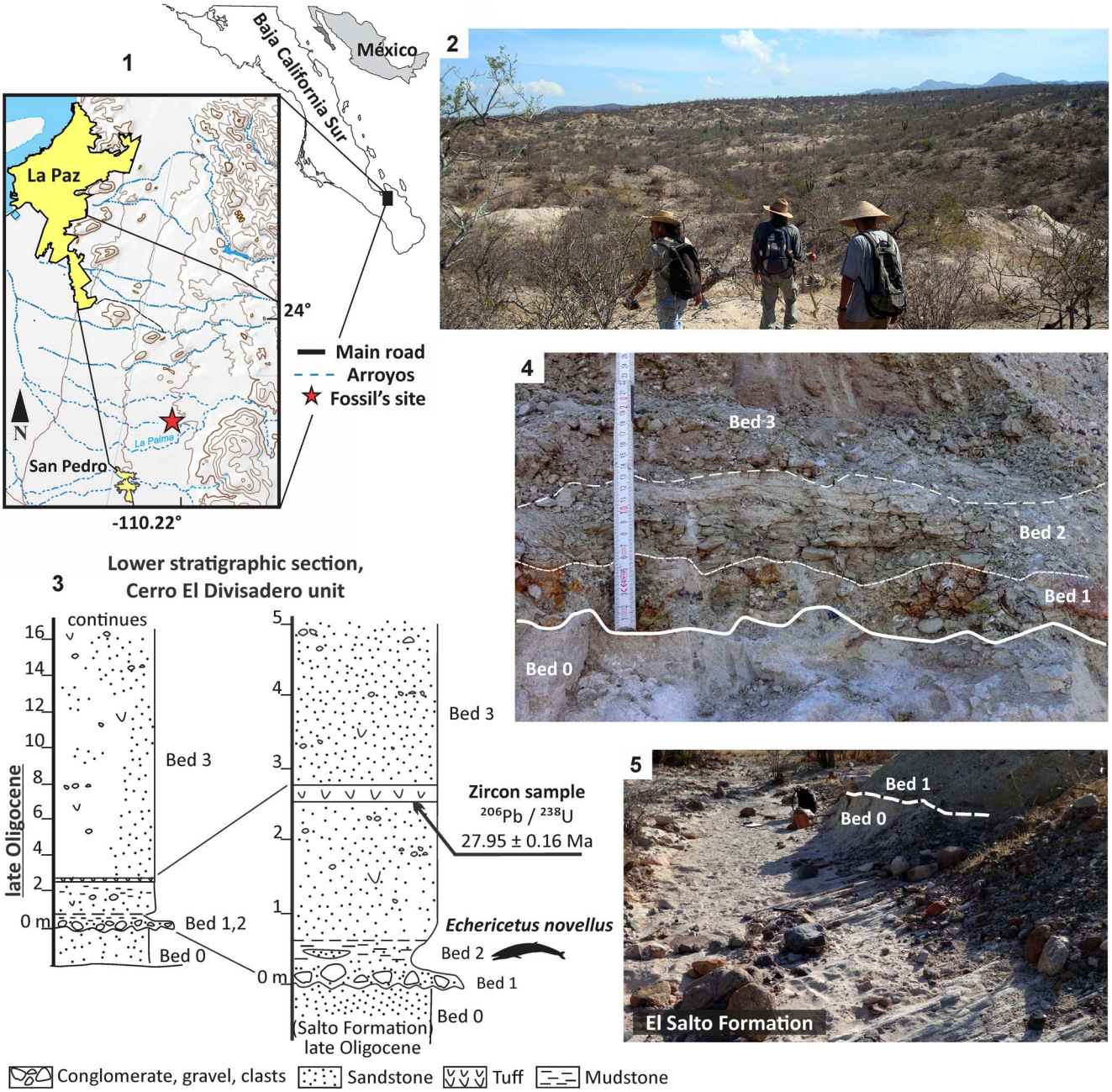

Figure 1. (**1**) Locality of *Echericetus novellus* n. gen. n. sp. (topographic map modified from INEGI, 2007, 2017). (**2**) Panoramic view at the Cerro El Divisadero locality. (**3**) Stratigraphic section. (**4, 5**) Details and contact of the lower strata with the Salto Formation (NAD 27 23°58'23"N, 110°13'42.4"W).

of the volcaniclastic arc-derived Comondú Group (Hausback, 1984; Drake et al., 2017).

Material and methods

The specimen MRAHBCS Pal/V119 (previously known as MRAHBCS 002; Hernández-Cisneros and Nava-Sánchez, 2022) is stored in the paleontological collection of the Museo Regional de Antropología e Historia de Baja California Sur, Baja California Sur, México. The preparation of MRAHBCS Pal/V119 included mechanical and chemical (bathed in 10% acetic acid) methods. Polyvinyl acetate was used to glue the fragmented pieces. After the preparation, photos were taken with a Nikon D3400 camera with an 18 mm lens. Anatomical terms follow Mead and Fordyce (2009). Data and remarks matrix for phylogenetic analysis and measurements can be found in the Supplemental files.

Phylogenetic analysis.—The phylogenetic analysis was performed on the basis of the original data matrix from Marx and Fordyce (2015), including recent updates from Hernández-Cisneros and Nava-Sánchez (2022) and Hernández-Cisneros (2022). We reviewed coded characters for *Maiabalaena* and *Sitsqwayk*, considering the observations from Boessenecker et al. (2023)

https://doi.org/10.1017/jpa.2023.80 Published online by Cambridge University Press

that suggest their inclusion in Eomysticetidae. The following characters were changed in both taxa: character (c.) 26 coded from the state (s.) "?" to s. "1" (teeth in adult individuals absent or vestigial; see discussion on baleen origins; Ekdale and Deméré, 2022; Gatesy et al., 2022); c. 83 from s. "2" to s. "1" (the temporal fossa form a large parasagittal oval); c. 100 from s. "0" to s. "2" (almost 90° twisting of the zygomatic process of squamosal). For *Maiabalaena*, c. 11 was changed from s. "?" to s. "1" (antorbital process present and defined by a steep face separating the posterolateral corner of the maxilla from its more anterior rostral portion); c. 103 from s. "0" to s. "1" (absent supramastoid crest of the zygomatic process of squamosal). For *Sitsqwayk*, c. 24 was changed from s. "?" to s. "1" (a straight facial portion of the rostrum in lateral view). In addition, the following characters in *Tlaxcallicetus guaycurae* Hernández-Cisneros, 2018 were changed: c. 83 from s. "2" to s. "?"; c. 99 from s. "0" to s. "?"; c. 117 from s. "2" to s. "1"; c. 119 from s. "1" to s. "0"; c. 132 from s. "1" to s. "0"; c. 136 from s. "0" to s. "1"; c. 160 from s. "0" to s. "?"; c. 161 from s. "0" to s. "?"; c. 187 from s. "0" to s. "0&1." The present matrix of 272 characters has 112 terminal taxa (see the Supplemental files). During the analysis, we inactivated unpublished taxa (not ready for re-examination) and poorly preserved species (e.g., *Willungacetus*). Thus, 106 taxa were treated under the parsimony analysis using T.N.T. v.1.5 software (Goloboff and Catalano, 2016). Characters were analyzed under equal and implied weights (under the standard value k = 3 and the calculated k = 28.18360 using the script "setk"; Goloboff, 1993; Goloboff et al., 2008, 2018), ordered and using a backbone constraint tree—force / (5 ((16 51) (33 (48 ((19 21) ((26 73) (24 (22 25)))))))). Settings include 10,000 random stepwise-addition replicates per tree, bisection reconnection (TBR) branch swapping with 10 trees per replicate and enforce constraints. The multiple most parsimonious trees were summarized under strict consensus. Support values were obtained by symmetric resampling based on 2,000 replicates and reported as GC frequency differences (Goloboff et al., 2003). Under equal weights, a second analysis was run due to overflow replications using saved trees in the memory from the first result. Only the consensus tree resulting from the implied weights (k = 28.18360) is explained regarding the specimen MRAHBCS Pal/V119.

Repository and institutional abbreviation.—MRAHBCS, Museo Regional de Antropología e Historia de Baja California Sur—Instituto Nacional de Antropología e Historia.

Systematic paleontology

Cetacea Brisson, 1762
Mysticeti Gray, 1864
Eomysticetidae Sanders and Barnes, 2002b
Echericetus new genus

Type species.—*Echericetus novellus* n. sp., by monotypy.

Diagnosis.—As the monotypic species.

Occurrence.—Oligocene (slightly older than 27.95 Ma, latest Rupelian), North Pacific.

Etymology.—*Echeri* means land, earth, or ground in Purepecha, a local language in Mexico; *cetus* indicates large sea creature in Greek.

Remarks.—*Echericetus* represents a new genus of the Eomysticetidae in the North Pacific. The other definite eomysticetid genus is *Yamatocetus* from the Oligocene of Japan, on the other side of the North Pacific. Interestingly, a recent phylogenetic analysis (Boessenecker et al., 2023) recognized the eomysticetid affinity of *Sitsqwayk* and *Maiabalaena*, and if this taxonomic interpretation proves to be correct, the eomysticetid diversity in the North Pacific is much higher than previously known. In addition, Hernández-Cisneros and Nava-Sanchez (2022) identified the existence of *Eomysticetus* from the Oligocene of Mexico, indicating the occurrences in both the Pacific and Atlantic oceans of this eomysticetid genus.

Echericetus novellus new species
Figures 2–16

Holotype.—MRAHBCS Pal/V119 includes a partial skull (fragmentary rostrum, cranium with periotics, mandibles, and several bone fragments) and postcranial elements (31 vertebrae, ribs, and forelimb). It is curated in the paleontological collection of the MRAHBCS.

Diagnosis.—*Echericetus novellus* n. gen. n. sp. displays the combination of eomysticetid diagnostic features (Sanders and Barnes, 2002a, b; Boessenecker and Fordyce, 2015a): the elongate intertemporal region; large and oval temporal fossa; occipital shield relatively posterior to the postorbital process of frontal; broad and high coronoid process; transversely compressed blade-like anterior process of the periotic. Further, *Echericetus novellus* differs from known eomysticetids in having dorsoventrally thickened orbital rim with rounded surface; reduced and inconspicuous postorbital process; preorbital process thicker than the postorbital process; wide and long intertemporal region; supraoccipital with anteroposteriorly convex surface; elongated and elliptical pterygoid sinus fossa; squared-like basioccipital crest; rectangular anterior process of the periotic in medial view; S-shaped mandible in lateral view and the axis vertebra with bilobed hypapophysis. *Echericetus novellus* also differs from *Sitsqwayk cornishorum* Peredo and Uhen, 2016 and *Maiabalaena nesbittae* Peredo et al., 2018 in lack of a prominent postorbital process, relatively thin orbital rim, concave dorsal surface of the supraoccipital, and straight nuchal crest; it differs from *Mauicetus parki* (Benham, 1937), *Horopeta umarere* Tsai and Fordyce, 2015b, *Whakakai waipata* Tsai and Fordyce, 2016, *Tlaxcallicetus*, and *Toipahautea waitaki* Tsai and Fordyce, 2018 in the lack of a massive body of the periotic; transversally thick or very thin, dorsally prominent anterior process. *Echericetus novellus* differs from the crown Mysticeti (Balaenidae,

https://doi.org/10.1017/jpa.2023.80 Published online by Cambridge University Press

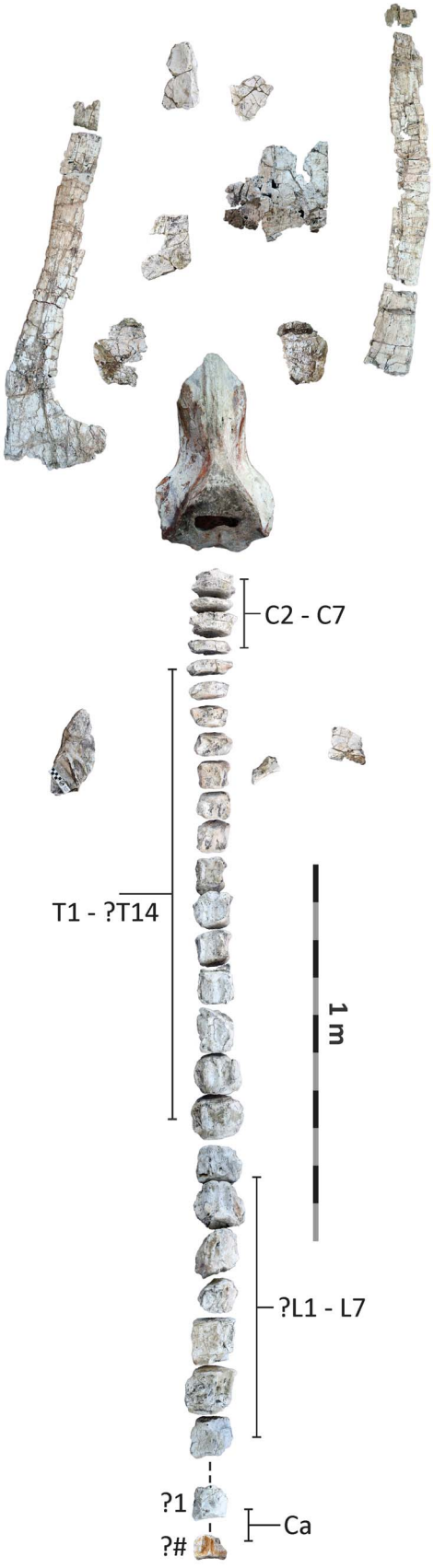

Figure 2. *Echericetus novellus* n. gen. n. sp., holotype, MRAHBCS Pal/V119; cervical vertebrae (C2–C7), thoracic vertebrae (T1–?T14), lumbar vertebrae (?L1–L7), and caudal vertebrae (Ca).

Balaenopteridae, Cetotheriidae, Eschrichtiidae) in having archaic features, such as a poorly telescoped skull, prominent plate-like coronoid process, the presence of the fovea epitubaria, and the acoustic meatus as a single aperture.

Occurrence.—Marine marginal facies, San Juan Member, El Cien Formation, ~20 km southeast of La Paz, Baja California Sur, Mexico, (NAD 27 23.973618°N, 110.228921°W), 1.2 km southwest of Sierra El Novillo, 500 m northwest of Rancho La Palma, and 500 m northeast of Cerro El Divisadero. Based on the lithology and the U–Pb zircon dating from the horizon slightly above MRAHBCS Pal/V119, the geological age for *Echericetus novellus* n. gen. n. sp. (bed 2; Fig. 1) is slightly older than 27.95 Ma (latest Rupelian).

Description.—Overall, the bioerosion of MRAHBCS Pal/V119 is minor, having relatively good preservation; some vertebrae show a degree of pre-burial degradation. The rostrum, mandibles, supraorbital processes of the frontal, and vertebrae display considerable distortion by the diagenetic processes. The bony fractures and loss of bones may be from weathering after exposure. The skull contains invertebrate shells (bivalves) in the pterygoid fossa and gypsum crystals inside the braincase cavity, which formed likely to the current desert climate.

Ontogenetic age and body size.—*Echericetus novellus* n. gen. n. sp. includes both mature and immature physical features (Walsh and Berta, 2011; Boessenecker and Fordyce, 2015a): open skull sutures that are not tightly fused (immature), well-fused vertebral epiphyses (mature), and closed occipital synchondroses (mature). Thus, the holotype MRAHBCS Pal/V119 likely represents a subadult. Judging from the preserved skull and mandibles, the total body length of *Echericetus novellus* may be comparable to *Tokarahia*, around 5 to 6 m long.

Skull.—*Echericetus novellus* n. gen. n. sp. preserves only fragments of the maxillae (Fig. 2), showing a flattened maxilla without alveoli (at least on the lateral borders posterior to the rostrum tip); no baleen is preserved. The frontal fragments indicate an exposed skull vertex, and the supraorbital processes have been preserved (Figs. 4, 5); the frontoparietal suture is not visible. The antorbital process is over the anterior end of the supraorbital process. The orbit is shorter than <25% of the bizygomatic width, and the orbital rim is dorsoventrally thick (26.4–31 mm, maximum) with a rounded lateral surface. The preorbital region is dorsoventrally flat; the postorbital process is not prominent, with a rounded tip oriented posteriorly. The postorbital process is dorsoventrally thinner (11.7 mm) than the preorbital process (16.5 mm). Above the supraorbital process, the orbitotemporal crest is indistinct with a swollen surface, which is oriented subparallel to the posterior border and indicates the limit of the insertion area for the temporalis muscle.

The anterior and lateral profiles of the cranium indicate an ascending angle >10° toward the posterior edge of the skull, showing the broken frontal at a level above the lateral border of the rostrum. Dorsally, the temporal fossa and the intertemporal region are anteroposteriorly longer than the transverse width. The parietals are posterior to the postorbital process, and part of the dorsal surface in the parietals has been lost (Figs. 5, 7, 8). The sagittal suture anterior to the supraoccipital apex is present. In lateral view, parietals are anteroposteriorly

https://doi.org/10.1017/jpa.2023.80 Published online by Cambridge University Press

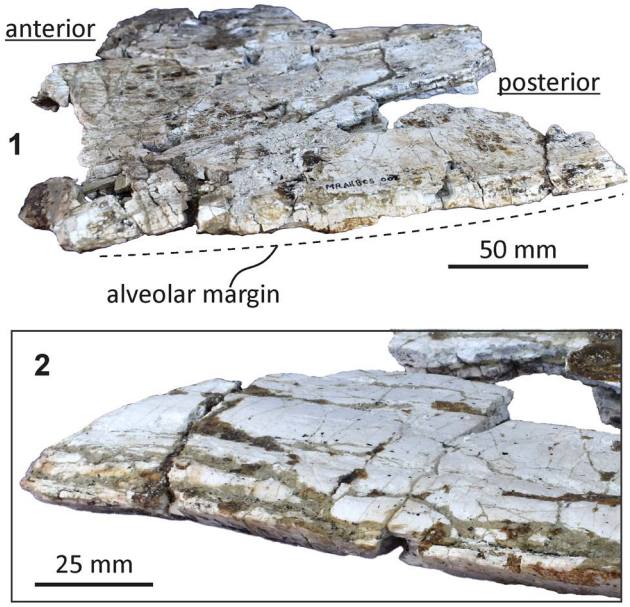

Figure 3. *Echericetus novellus*, holotype, MRAHBCS PAL/V118. (**1, 2**) Fragment of the right maxilla: (**1**) dorsal view; (**2**) ventral view.

longer than high and are in contact with the supraoccipital, resulting in the partial nuchal crest. Ventrally, the parietal contacts and fuses with the alisphenoid and orbitosphenoid. The suture of the parietal–squamosal joint is smooth and orients obliquely without tubercles or foramen.

As in other stem mysticetes, the apex of the supraoccipital is located posterior to the postorbital process and directly posterior to the exposed parietals. In *Echericetus novellus* n. gen. n. sp., the anteriormost point of the supraoccipital is within the temporal fossa and likely posterior to the zygomatic process tip. The preserved supraoccipital indicates a broadly rounded anterior margin. The nuchal crest is convex in dorsal view. The supraoccipital outline is triangular in dorsal view. The posterior apex of the nuchal crest is anterior to the occipital condyles and aligned with the medial half of the temporal fossa. The nuchal crest seems not to overhang the squamosal fossa. Dorsally, the supraoccipital lacks paired tubercles, and both lateral margins of the nuchal crest in dorsal view are slightly convex. The external occipital crest is present mainly over the posterior half of the supraoccipital and ends slightly anterior to the foramen magnum. In posterior view, the exoccipital is partially preserved and well fused with the supraoccipital. The condyles are present but eroded; the foramen magnum is circular. Ventrally, the exoccipital contributes to the narrow jugular notch and is fused with the basioccipital. In ventral view, the basioccipital and basisphenoid (basioccipital/basisphenoid synchondrosis) are well fused (Fig. 6), and the incomplete nasal plate of the vomer overlies the basisphenoid and contacts the basioccipital. The basioccipital crests are broad, bulbous (slightly eroded), and subparallel to the sagittal plane, with a square-like outline and a straight lateral border.

The preserved portion of the squamosal is lateral to the parietal and supraoccipital. The dorsomedial surface of the squamosal is slightly convex and smooth without elevation, and the more lateral portion indicates a relatively narrow squamosal fossa. Ventrally, the medial portion of the incomplete squamosal belongs to the lateral part of the pterygoid sinus fossa and includes the ventral opening of the foramen ovale. The pterygoid is exposed ventrally and is not well preserved. The pterygoid, squamosal, and basioccipital mark the outline of a long and elliptic pterygoid sinus fossa anterior to the foramen ovale. Most of the sphenoid bones are poorly preserved. The alisphenoid is broadly exposed laterally and contacts anteriorly with the eroded orbitosphenoid and dorsally with the parietal; the

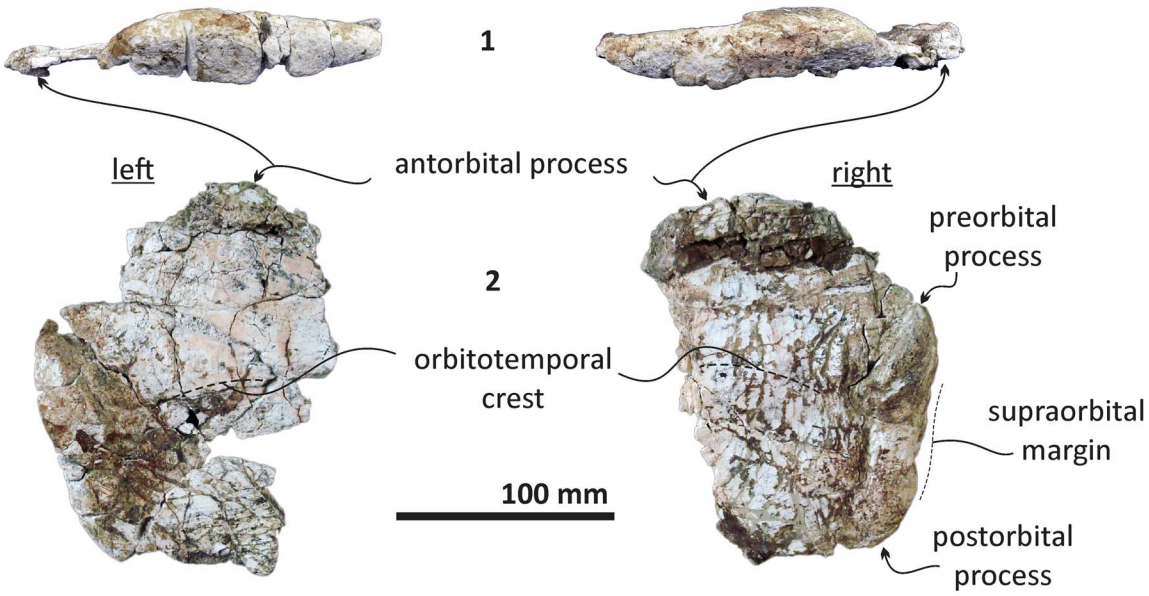

Figure 4. *Echericetus novellus* n. gen. n. sp., holotype, MRAHBCS Pal/V119. (**1, 2**) Supraorbital processes: (**1**) lateral view; (**2**) dorsal view.

https://doi.org/10.1017/jpa.2023.80 Published online by Cambridge University Press

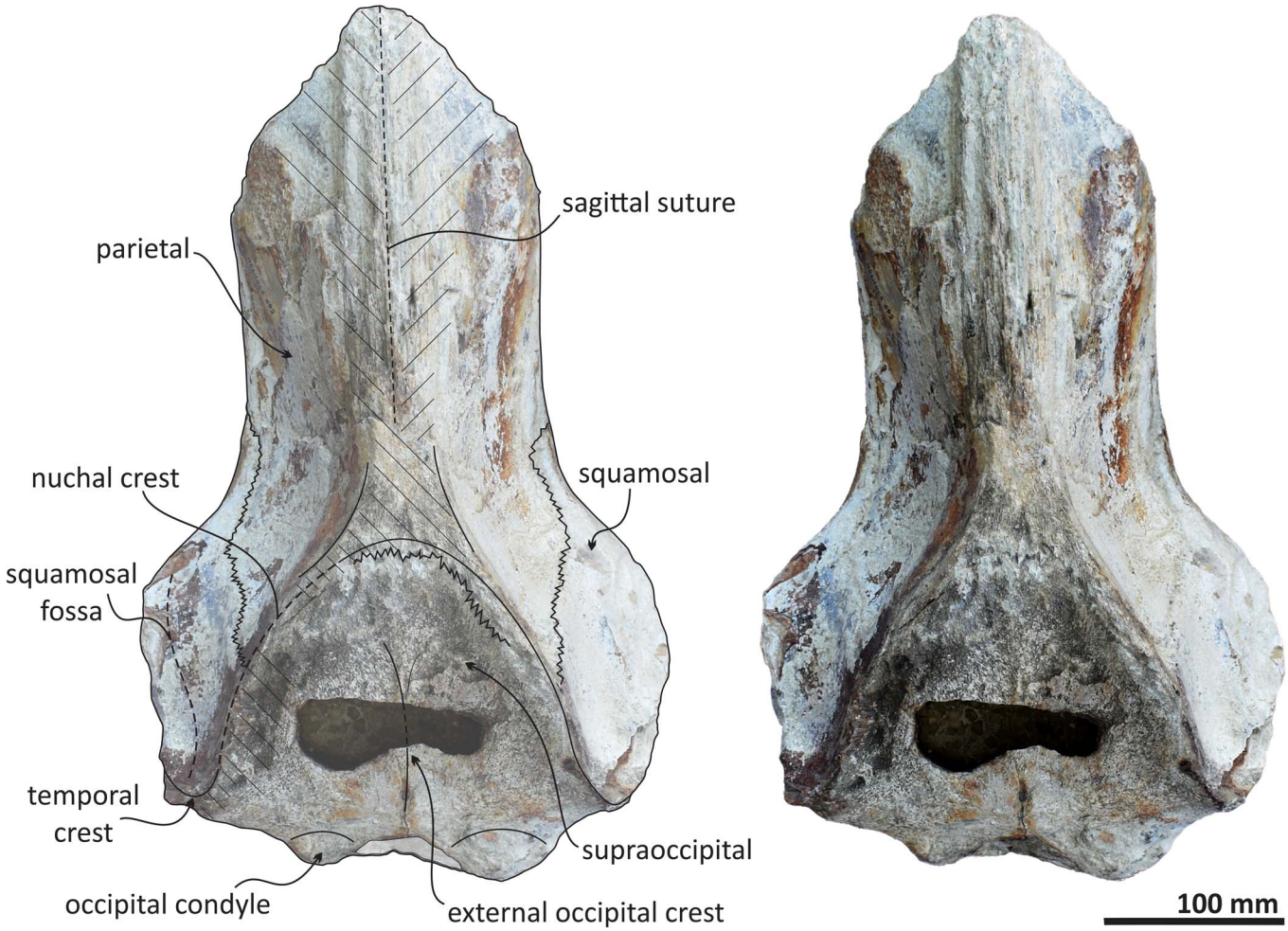

Figure 5. *Echericetus novellus* n. gen. n. sp., holotype, MRAHBCS Pal/V119, cranium, dorsal view. Crosslines denote broken or eroded surface.

exposed and remaining alisphenoid is anteroposteriorly elongated and rectangular in lateral view. The basisphenoid is visible in the palatine region and well fused posteriorly with the basioccipital. Fragments of the vomer (including nasal plates and crest) cover part of the basisphenoid.

Periotic.—MRAHBCS Pal/V119 preserves two periotics, but only the right one was prepared to show the morphological features (Figs. 11, 12). The anterior, medial, and posterior views of the periotic are observable. Still, the dorsal surface with the suprameatal area, superior process, and vestibular and cochlear aqueducts are not visible (covered by the matrix). In medial view, the anterior process is rectangular and separated from the pars cochlearis; the incisural flange is present. The keel is mainly vertical, the anterodorsal angle is not exposed, and the anteroventral angle shows a blunt tip at the level of the ventral edge of the pars cochlearis. In ventral view, the anterior process is compressed transversely with a blade-like shape and lacks secondary tuberosity, and the anterior bullar facet forms an elongated triangle on the ventral surface of the anterior process. The fovea epitubaria is an eroded small area, indicating an accessory ossicle for the contact between the anterior process and bulla. The anterior process length is smaller than the anteroposterior length of the pars cochlearis. The lateral side remains embedded, but the anteroexternal sulcus is present and observable from the ventral rim of the artery channel. In medial view, a minor excavation above the fovea epitubaria marks the surface for the tensor tympani.

The pars cochlearis lacks a cranial elongation and shows a rounded surface at the anteromedial corner with a short ridge below the shallow promontorial groove in ventral view. Anterior and separated from the internal auditory meatus, a small fissure marks the opening of the hiatus fallopii. The posterior region of the pars cochlearis displays a small caudal tympanic process, which is triangular and well separated from the facial crest (crista parotica). In the rounded posteromedial corner, the fenestra rotunda is a circular opening with three small furrows in the dorsal edge separated from the rounded cochlear aqueduct. In ventral view, the small and round lateral tuberosity is anterolateral to the well-excavated mallear fossa; the body of the periotic is not prominent, and the area of the hiatus epitympanicus can be observed posterior to the mallear fossa. The fossa incudis is indistinct. The facial crest forms the lateral border of the opening of the facial canal, facial sulcus, and the fossa for the stapedius muscle. The medial surface close to the fenestra ovalis is not prominent. The posterior process is broken and oriented posterolaterally. The texture of the posterior process is dense and lacks a neck.

https://doi.org/10.1017/jpa.2023.80 Published online by Cambridge University Press

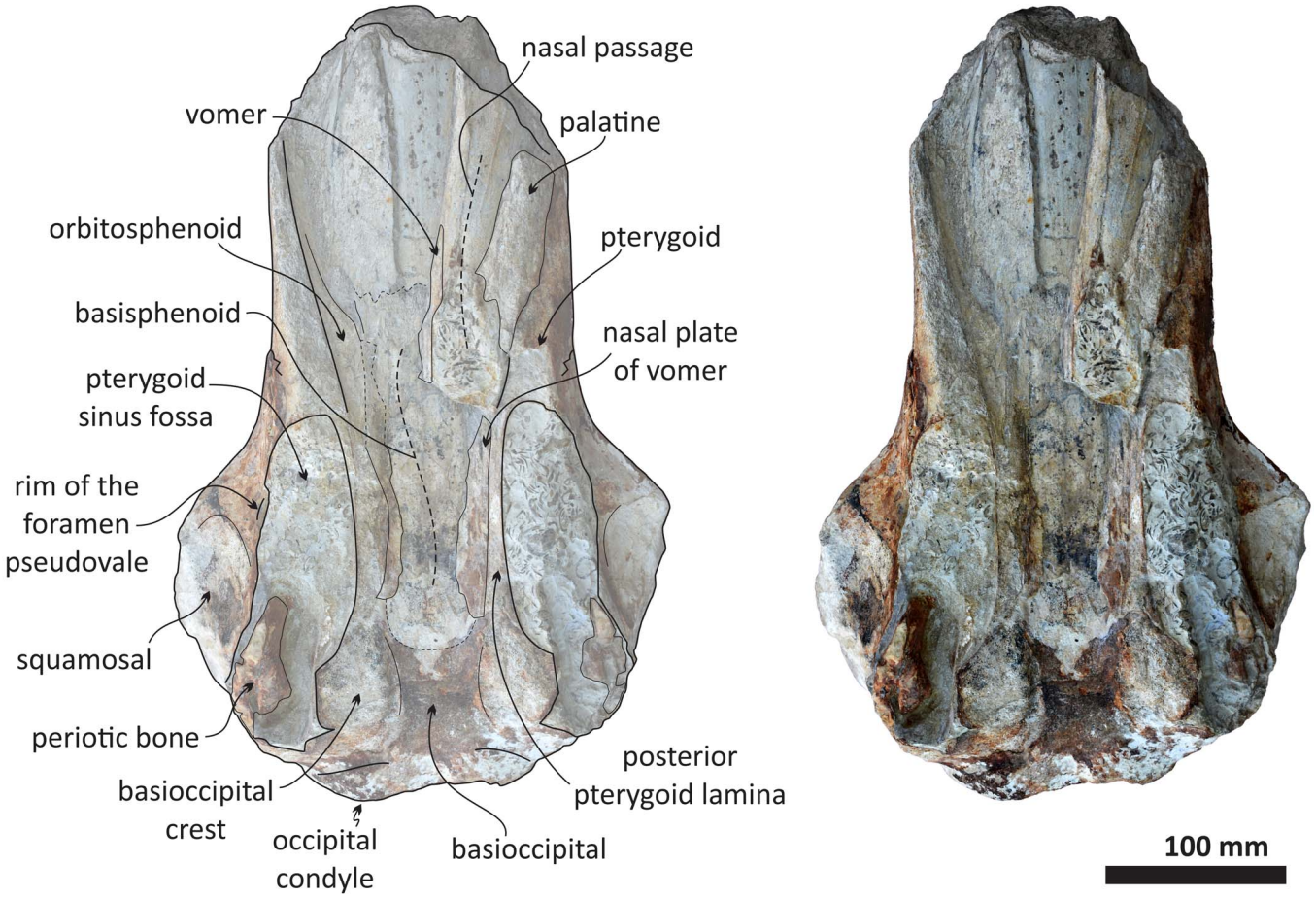

Figure 6. *Echericetus novellus* n. gen. n. sp., holotype, MRAHBCS Pal/V119, cranium, ventral view.

Mandible.—The mandibles are partially preserved; the anterior tip, the articular surface, and the angular process are missing. The diagenetic processes likely transformed the mandibular morphology slightly; we prudently interpreted the morphology and reconstructed the outline in dorsal view (Figs. 12, 13). The mandible is not straight in lateral view, distinct to *Eomysticetus*, *Yamatocetus*, *Tokarahia*, and *Waharoa.* The overall mandibular shape resembles that of *Sitsqwayk cornishorum*. Both mandibles are transversely compressed, and the left mandible displays more alteration, including a completely flat coronoid process and a distorted mandibular body. The preserved dorsal surface of the mandibles and the preserved maxilla indicate that *Echericetus novellus* n. gen. n. sp. lacks both functional teeth and alveolar grooves. Despite the absence of the mandibular tip, we suggest that *Echericetus novellus* has an unfused mandibular symphysis. The mandible preserves a flattened medial surface in the central part relative to the lateral surface. The ramus shows a flat dorsomedial surface, and the mandibular body of the right mandible displays a central constriction, like in aetiocetids, *Sitsqwayk*, and *Maiabalaena*. In dorsal view, the right mandible is bowed laterally, but mainly at the anterior portion. The medial wall of the broad mandibular foramen is broken, but the preserved mandibular foramen shows a rounded opening and at the base of the coronoid process. The medial projection on the dorsal margin and the satellite process are absent. The mandibular fossa is incomplete. The coronoid process is a transversely thin plate and lacks a posteromedial ridge and postcoronoid elevation. The insertion area for the mylohyoid muscle is absent.

Vertebrae.—MRAHBCS Pal/V119 includes 31 partially preserved vertebrae (Figs. 14, 15). The identification and probable arrangement of the vertebrae are based on the criteria and comments by Watson and Fordyce (1993; *Balaenoptera acutorostrata*), Okazaki (2012; *Yamatocetus canaliculatus*), Martínez-Cáceres et al. (2017; *Cynthiacetus peruvianus*), and de Muizon et al. (2019; *Mystacodon selenensis*). In general, the body of the vertebrae (anterior epiphysis, centrum, and posterior epiphysis) is relatively complete, although the diagenesis and erosion are evident on the MRAHBCS Pal/V119 vertebrae set. Only six of seven cervical vertebrae are preserved (from the axis to the seventh cervical vertebrae). The cervical vertebrae are unfused and display a rounded body. Still, some seem fused due to the diagenetic process. The axis has the odontoid process and a bi-lobed hypapophysis. Note that the atlas and axis have an exceptionally distinct morphology (Martínez-Cáceres et al., 2017). The other cervical vertebrae display a relatively anteroposteriorly flat body, and the characteristic parapophysis is absent in the thoracic, lumbar, and caudal vertebrae (Watson and Fordyce, 1993; Martínez-Cáceres et al., 2017). In *Echericetus novellus* n. gen. n. sp., many features are lost in the cervical

https://doi.org/10.1017/jpa.2023.80 Published online by Cambridge University Press

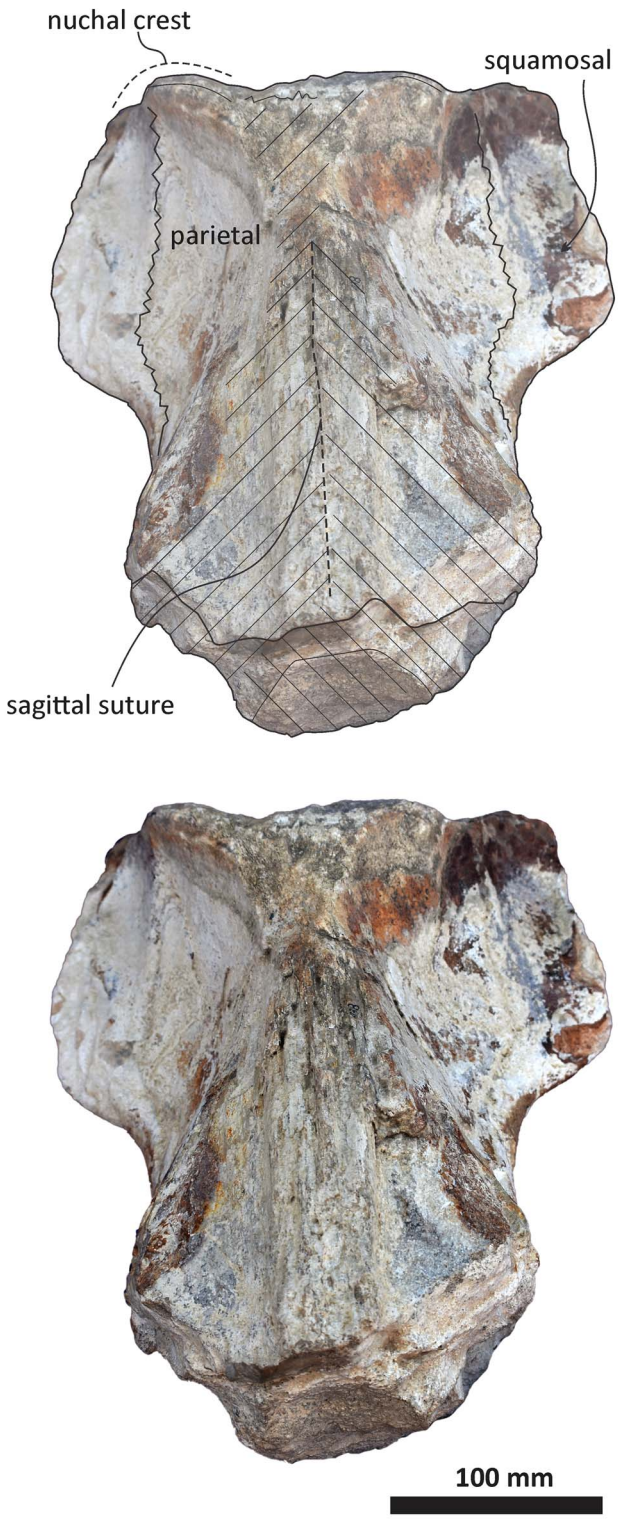

Figure 7. *Echericetus novellus* n. gen. n. sp., holotype, MRAHBCS PAL/V118, cranium, anterior view. Crosslines denote broken or eroded surface.

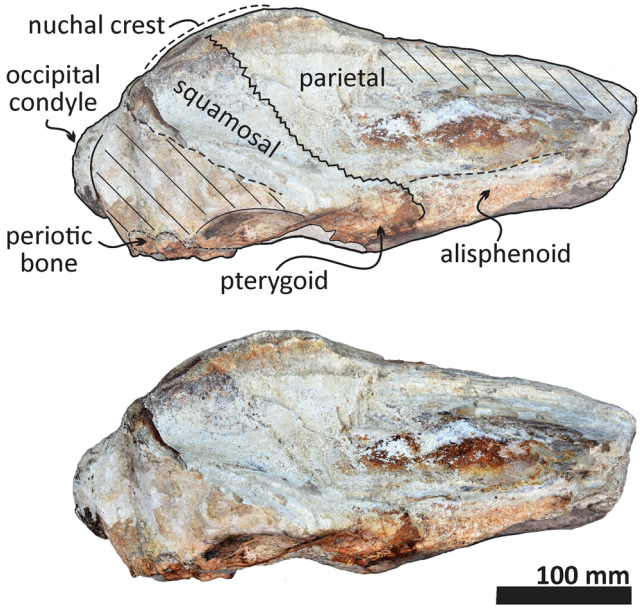

Figure 8. *Echericetus novellus* n. gen. n. sp., holotype, MRAHBCS PAL/V118, cranium, lateral view. Crosslines denote broken or eroded surface.

vertebrae due to erosion and diagenetic alterations. However, the vertebrae order was based on the preserved trace of the parapophysis and the vertebral body shape comparable to the *Yamatocetus canaliculatus* vertebrae set (Okazaki, 2012). Similar criteria were followed to order the thoracic vertebrae despite the poor preservation. Thus, the traces of the pedicle position, the presence of the fovea for the capitulum of the rib, the absence of the transverse process on the lateral wall of the vertebrae body in the first twelve thoracic vertebrae, and the thickness of the transverse process in the thoracic vertebrae 13 and ?14 (different from the flat and wide transverse process in lumbar vertebrae) allow the identification (Okazaki, 2012; Martínez-Cáceres et al., 2017; de Muizon et al., 2019). The lumbar and caudal vertebrae are more eroded and diagenetically altered; the order remains uncertain. In the case of the documented lumbar vertebrae, we suggest that they are likely the first seven vertebrae, considering the vertebrae body shape and traces of the transverse process base (Okazaki, 2012; Martínez-Cáceres et al., 2017; de Muizon et al., 2019). The lateral processes of the lumbar vertebrae show a subhorizontal orientation. The caudal vertebrae were interpreted on the basis of the preserved morphology, but again, the order remains uncertain. No detailed field notes for MRAHBCS Pal/V119 were recorded during the collecting process.

Forelimb.—MRAHBCS Pal/V119 includes the distal portion of the right scapula (Fig. 16), showing the glenoid fossa for articulating the humerus. The articulating surfaces of the left humerus, ulna, and radius are preserved. The olecranon process is broken, but the ulnar facet is shorter than the radial facet.

Etymology.—The specific name *novellus* (Latin for youth, new) alludes to the Sierra El Novillo, a mountain complex east of the locality where the holotype was found south of La Paz, Baja California Sur, Mexico.

Remarks.—Both *Sitsqwayk cornishorum* and *Maiabalaena nesbittae*, also recovered in the northeastern Pacific, likely belong to eomysticetids (Boessenecker et al., 2023; this study). In addition, a recent paper identified the existence of *Eomysticetus* sp. from the Oligocene of Mexico. If all

https://doi.org/10.1017/jpa.2023.80 Published online by Cambridge University Press

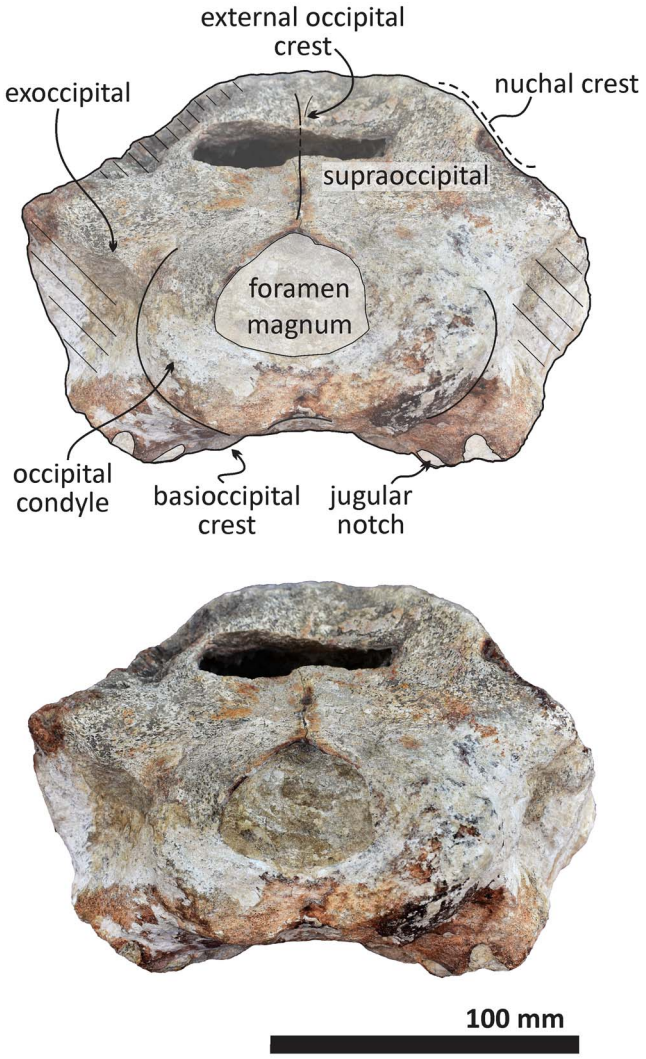

Figure 9. *Echericetus novellus* n. gen. n. sp., holotype, MRAHBCS PAL/V118, cranium, posterior view. Crosslines denote broken or eroded surface.

taxonomic identifications are correct, our *Echericetus novellus* n. gen. n. sp. and the previously known eomysticetid diversity in the northeastern Pacific become comparable to the South Pacific assemblage.

Phylogenetic analysis

Our consensus trees (Fig. 17), with the addition of *Echericetus novellus* n. gen. n. sp., is broadly similar to previous phylogenetic analyses (Marx and Fordyce, 2015; Fordyce and Marx, 2018; Peredo and Pyenson, 2018). Noteworthy, the recent inclusion of new stem mysticetes has provoked a substantial change in the phylogenetic relationships (see Fordyce and Marx, 2018; Schipps et al., 2019; Boessenecker et al., 2023; also see phylogenies based on problematic *Kekenodon*, Corrie and Fordyce, 2022). In our analyses, we test the phylogenetic relationship of *Echericetus novellus* n. gen. n. sp. regarding Eomysticetidae under three different criteria related to the concavity value of k, default value 3 and the calculated value 28.18360, and equal weights criteria (k "determines how strongly homoplasious characters are down-weighted"; Goloboff, 1993; Goloboff et al., 2008, 2018). Only the consensus tree under the value k = 28.18360 is described (the preferred tree; Fig. 17.1), and the other trees are used to show alternative topologies (Fig. 17). A broad review or discussion on Mysticeti phylogeny is beyond the scope of this study. Similarly, our preferred tree (Fig. 17.1) also supports the recently suggested inclusion of *Sitsqwayk* and *Maiabalaena* in Eomysticetidae (Boessenecker et al., 2023). In a broad sense, Coronodonidae, Llanocetidae, and Mammalodontidae have been clustered with Odontoceti (Fig. 17), suggesting that the relationships among early neocete evolution remain problematic (also see Corrie and Fordyce, 2022 for similar results). Problematic taxa such as Coronodonidae (Boessenecker et al., 2023), *Mystacodon* and *Llanocetus* (Llanocetidae, sensu Fordyce and Marx, 2018), *Tlaxcallicetus* and *Mauicetus* (crownward mysticetes) show various phylogenetic positions, depending on the chosen criteria. Thus, such contradictions might result from missing data (morphology and taxa). Among Chaeomysticeti, eomysticetids are the most basal chaeomysticetes diverging after the toothed mysticetes. In addition, under implied weights (k = 28.18360; Fig. 17.1), the position of *Maiabalaena* + *Sitsqwayk* differs from previous results (Peredo et al., 2018) and conforms to the result of Boessenecker et al. (2023): both *Maiabalaena* and *Sitsqwayk* are eomysticetids. Interestingly, our result also shows that *Maiabalaena* and *Sitsqwayk* may be diverging earlier than eomysticetids under equal weights (Fig. 17.2) or more derived than eomysticetids under implied weights (Fig. 17.3).

On the basis of the consensus tree under implied weights (k = 28.18360; Fig. 17.1) from the nine most parsimonious trees, the synapomorphies support the inclusion of *Maiabalaena* and *Sitsqwayk* within Eomysticetidae: anteriormost point of palatine located anterior to the level of the antorbital notch (c. 21/s. 1; coded only in *Yamatocetus*); the temporal fossa forms a large parasagittal oval (c. 83/s. 1; such a character might be interpreted and coded differently due to disparity and ontogenetic variants; here all the taxa share this character); highly irregular outline of the frontoparietal suture (c. 86/s. 2; different in *Maiabalaena*); an extremely well-developed and robust zygomatic process of squamosal (c. 96/s. 1; present in almost all the taxa); anterior process transversely compressed and blade-like (c. 150/s. 1; unknown in *Sitsqwayk*); subcondylar furrow as a medially well-defined groove with the dorsal border being accentuated by a medially well-developed condyle (c. 228/s. 2; coded only in *Maiabalaena* + *Sitsqwayk* and different in *Yamatocetus*); the apices of neural spines of posterior thoracic and anterior lumbar vertebrae anteroposteriorly expanded and squared off (c. 247/s. 1; unknown in more than half of taxa). Our analysis under implied weights (k = 28.18360; Fig. 17.1) differs from the results of Boessenecker et al. (2023) in that the branch of *Maiabalaena* + *Sitsqwayk* and eomysticetids has a branch support of less than 50%. However, our dataset differs from that of Boessenecker et al. (2023), but both datasets consistently recover that *Maiabalaena* and *Sitsqwayk* are eomysticetids. New materials of *Maiabalaena* and *Sitsqwayk* should further reveal the eomysticetid affinity and resolve the relationships within Eomysticetidae.

Last, *Echericetus novellus* n. gen. n. sp. is also an eomysticetid, based on 86 characters (31.6% of the matrix). The relationships of *Echericetus novellus* with other eomysticetid

https://doi.org/10.1017/jpa.2023.80 Published online by Cambridge University Press

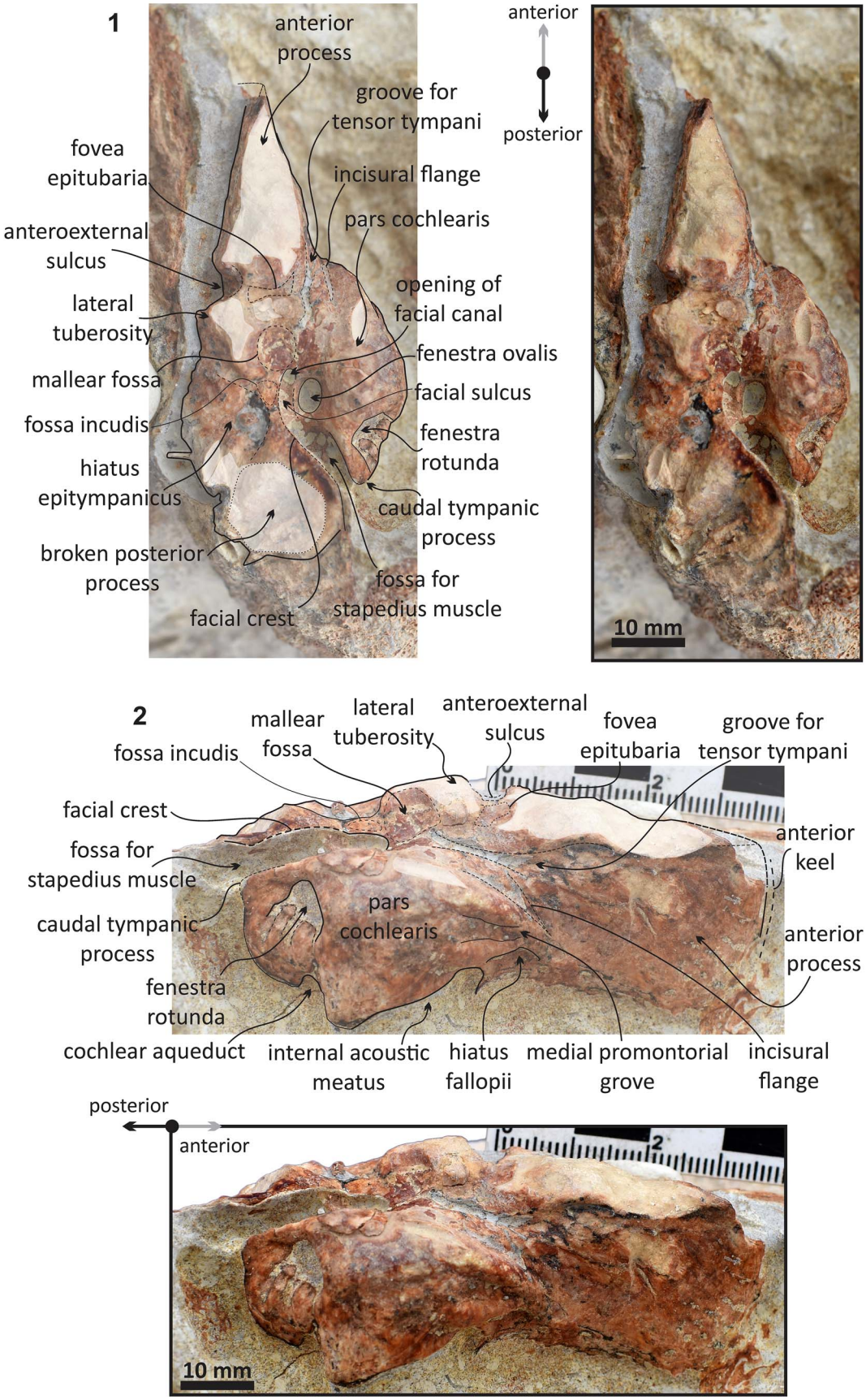

Figure 10. *Echericetus novellus* n. gen. n. sp., holotype, MRAHBCS Pal/V119. (**1, 2**) Right periotic: (**1**) ventral view; (**2**) medial view.

https://doi.org/10.1017/jpa.2023.80 Published online by Cambridge University Press

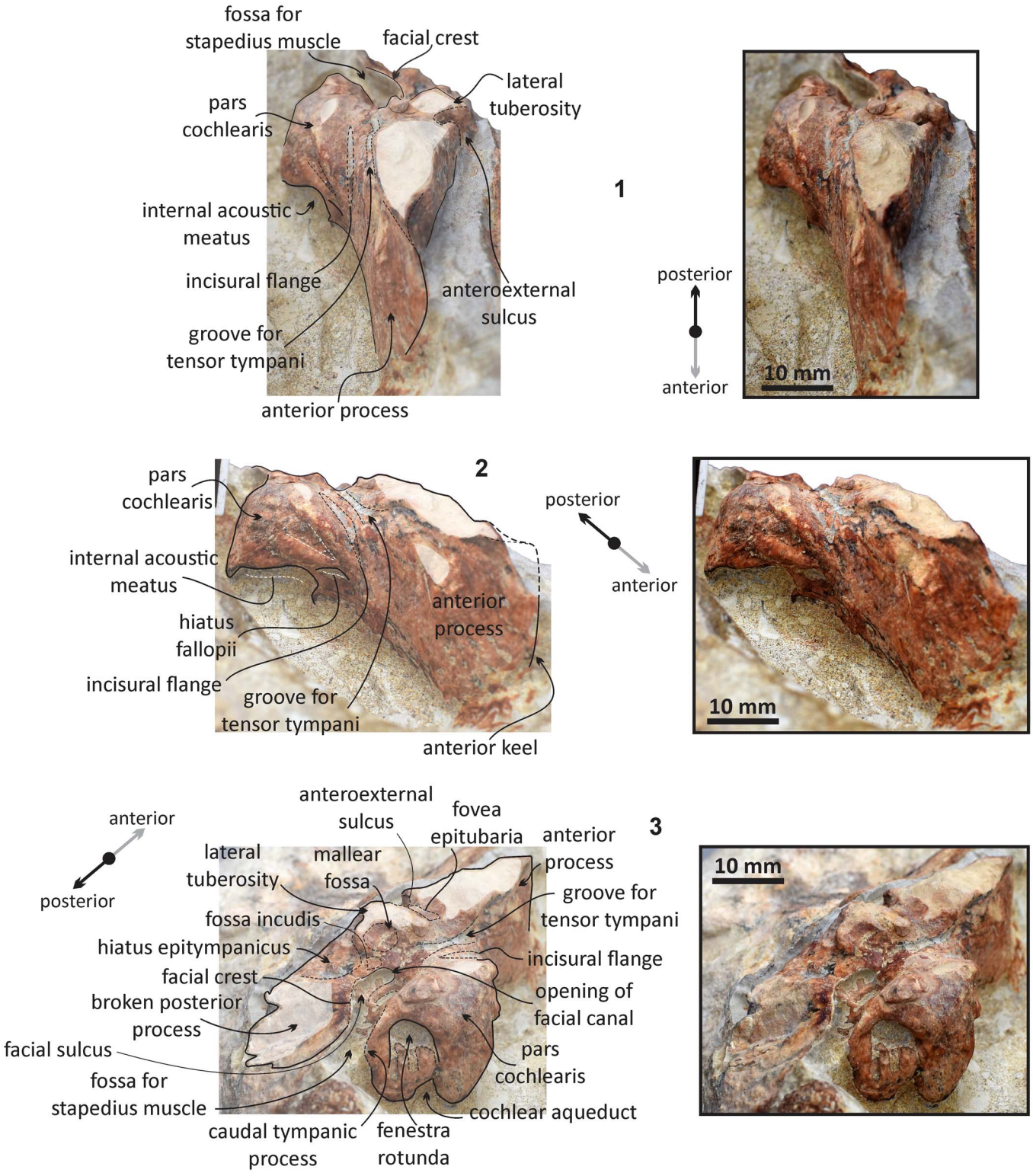

Figure 11. *Echericetus novellus* n. gen. n. sp., holotype, MRAHBCS Pal/V119. (**1–3**) Right periotic: (**1**) anterior view; (**2**) anteromedial view; (**3**) posteromedial view.

remain unresolved. Here, *Echericetus novellus* forms a polytomy with *Yamatocetus*, *Micromysticetus*, and *Eomysticetus* (Fig. 17.1). The branch that indicates the relationship of *Echericetus novellus* with six eomysticetid genera has 59% support. The recovered synapomorphies for this branch are an extended rostral portion of maxilla anterior to antorbital notch with more than one and a half times the bizygomatic width (c. 1/s. 2); transverse width of maxilla at midpoint with more than twice the width of the premaxilla (c. 5/s. 2); apex of the zygomatic process of squamosal deflected anteroventrally (c. 102/s. 1);

https://doi.org/10.1017/jpa.2023.80 Published online by Cambridge University Press

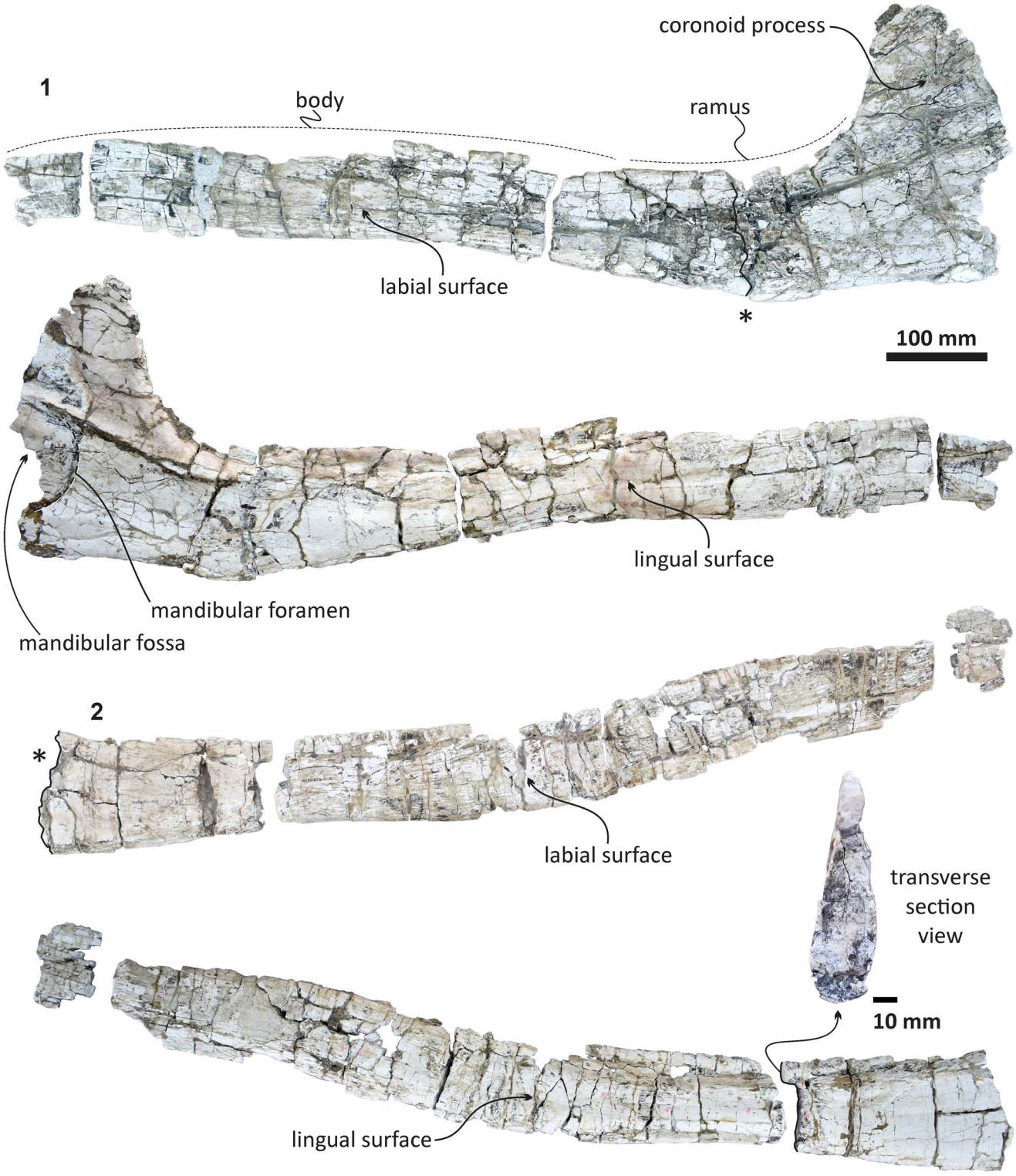

Figure 12. *Echericetus novellus* n. gen. n. sp., holotype, MRAHBCS Pal/V119. (**1**) Left mandible. (**2**) Right mandible. The asterisks mark the equivalent section level at the right mandible.

posteriormost point of exoccipital located more anteriorly than the posterior edge of the occipital condyle (c. 139/s. 0); medial lobe of tympanic bulla subequal in width to the lateral lobe or smaller (c. 202/s. 1); subcondylar furrow as a medially well-defined groove with the dorsal border being accentuated by a medially well-developed condyle (c. 228/s. 2); the height of transverse process of the atlas at the base equal to half the height of the articular surface or less (c. 239/s. 1). The autapomorphies of *Echericetus novellus* n. gen. n. sp. are postorbital process short and not markedly projecting in any direction (c.

https://doi.org/10.1017/jpa.2023.80 Published online by Cambridge University Press

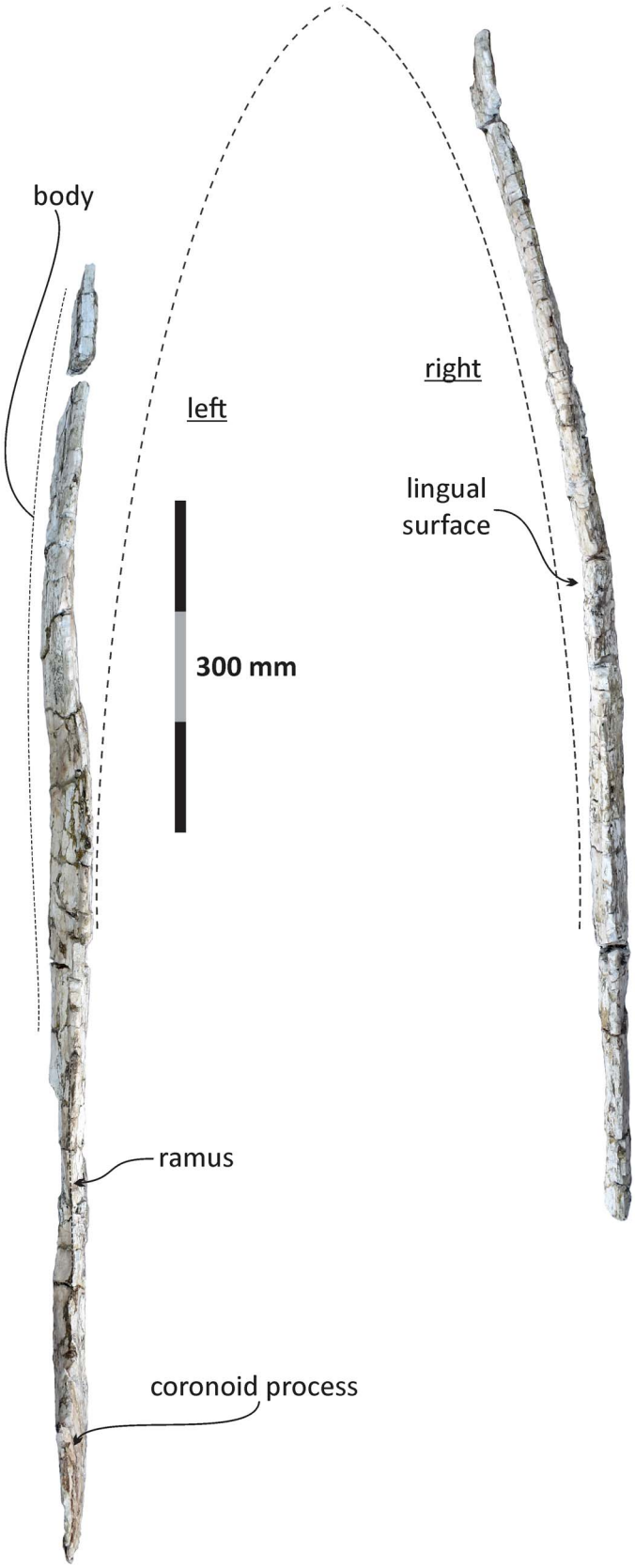

Figure 13. *Echericetus novellus* n. gen. n. sp., holotype, MRAHBCS PAL/V118, mandibles, dorsal view. The dashed line represents the reconstructed outline.

https://doi.org/10.1017/jpa.2023.80 Published online by Cambridge University Press

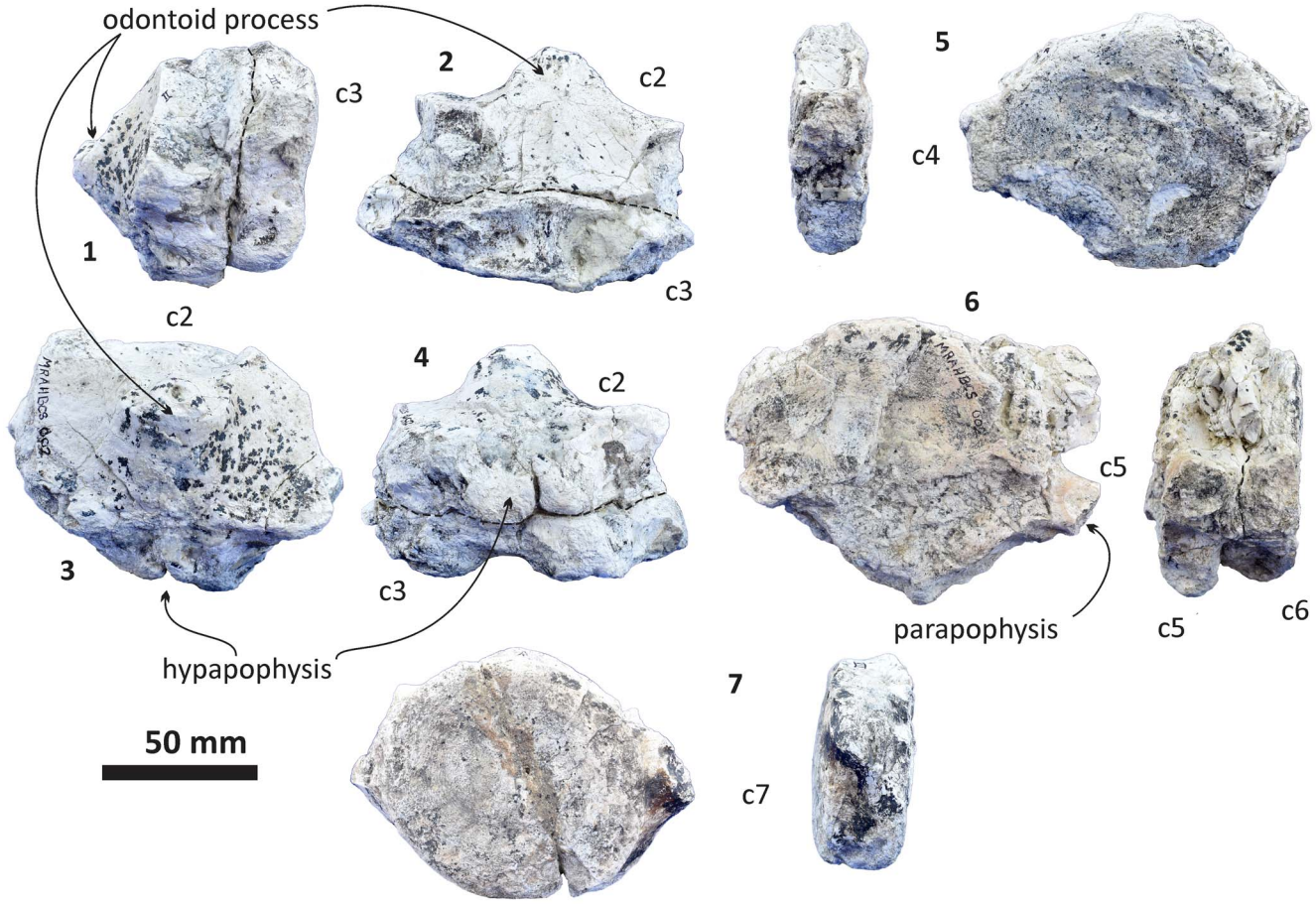

Figure 14. *Echericetus novellus* n. gen. n. sp., holotype, MRAHBCS Pal/V119, cervical vertebrae. (**1–4**) Axis (fused with the c3): (**1**) lateral view; (**2**) dorsal view; (**3**) anterior view; (**4**) ventral view. (**5**) Lateral and anterior views of the fourth cervical vertebra. (**6**) Fused cervical vertebra (c5–6), anterior and lateral views. (**7**) Anterior and lateral views of the seventh cervical vertebrae.

48/s. 3); the orbital rim of supraorbital process of frontal thickened with a rounded lateral surface (c. 50/s. 2); preorbital region of frontal dorsoventrally flat (c. 61/s. 1); flat or convex anterior half of dorsal surface of supraoccipital (c. 115/s. 1); absent distinct ridge delimiting insertion surface of tensor tympani on the medial side of anterior process but with an insertion surface distinctly excavated (c. 160/s. 1); well developed and large hiatus fallopii located anterior to proximal opening of the facial canal (c. 178/s. 1).

Discussion

The discovery of *Echericetus novellus* n. gen. n. sp. from the Oligocene of Mexico (slightly older than 27.95 Ma, latest Rupelian) adds to the growing list of new eomysticetids in the North Pacific (e.g., Hernández-Cisneros and Nava-Sánchez, 2022). The eomysticetid fossil record represents one of the best-sampled stem mysticete clades, but large-scale questions remain, such as the origin, adaptive traits, and functional morphology (whether eomysticetids were skim feeders, similar to right baleen whales), and the causes that drove their extinction after the Oligocene–Miocene transition (Boessenecker and Fordyce, 2015b, 2017b). The oldest eomysticetid fossils are *Micromysticetus rothauseni* and *Yamatocetus canaliculatus*, close to 30 Ma (Marx and Fordyce, 2015), whereas the youngest geological occurrence is the early Miocene *Waharoa* (~22.28 Ma, Aquitanian; Boessenecker and Fordyce, 2017b; also see Boessenecker, 2022), indicating that eomysticetids thrived at least for 8 to 11 Myr. Not only the longevity of eomysticetid lineage but also the high disparity and diversity, at least nine genera and 13 species (including *Echericetus novellus* n. gen. n. sp.; but also see Boessenecker and Fordyce, 2017a for a review of Eomysticetidae), suggest that eomysticetids represent an ecologically competitive and successful lineage. The wide distribution in the Pacific, Atlantic, and likely Mediterranean–Paratethys oceans indicates that eomysticetids likely responded to environmental pressures and relocated with food sources efficiently (Boessenecker and Fordyce, 2017b; Marx et al., 2019; Hernández-Cisneros and Nava-Sánchez, 2022), but the sudden disappearance of eomysticetids remains uncertain and likely opens up the ecological niches for the success of the "modern" mysticetes.

The environmental change during the Oligocene–Miocene boundary restructured the coastlines, likely leading to the demise of coastal cetacean species (e.g., aetiocetids and mammalodontids). Still, pelagic cetaceans, such as eomysticetids, presumably were not highly affected (Marx et al., 2019). As a possible transitional form between toothed and baleen-bearing

https://doi.org/10.1017/jpa.2023.80 Published online by Cambridge University Press

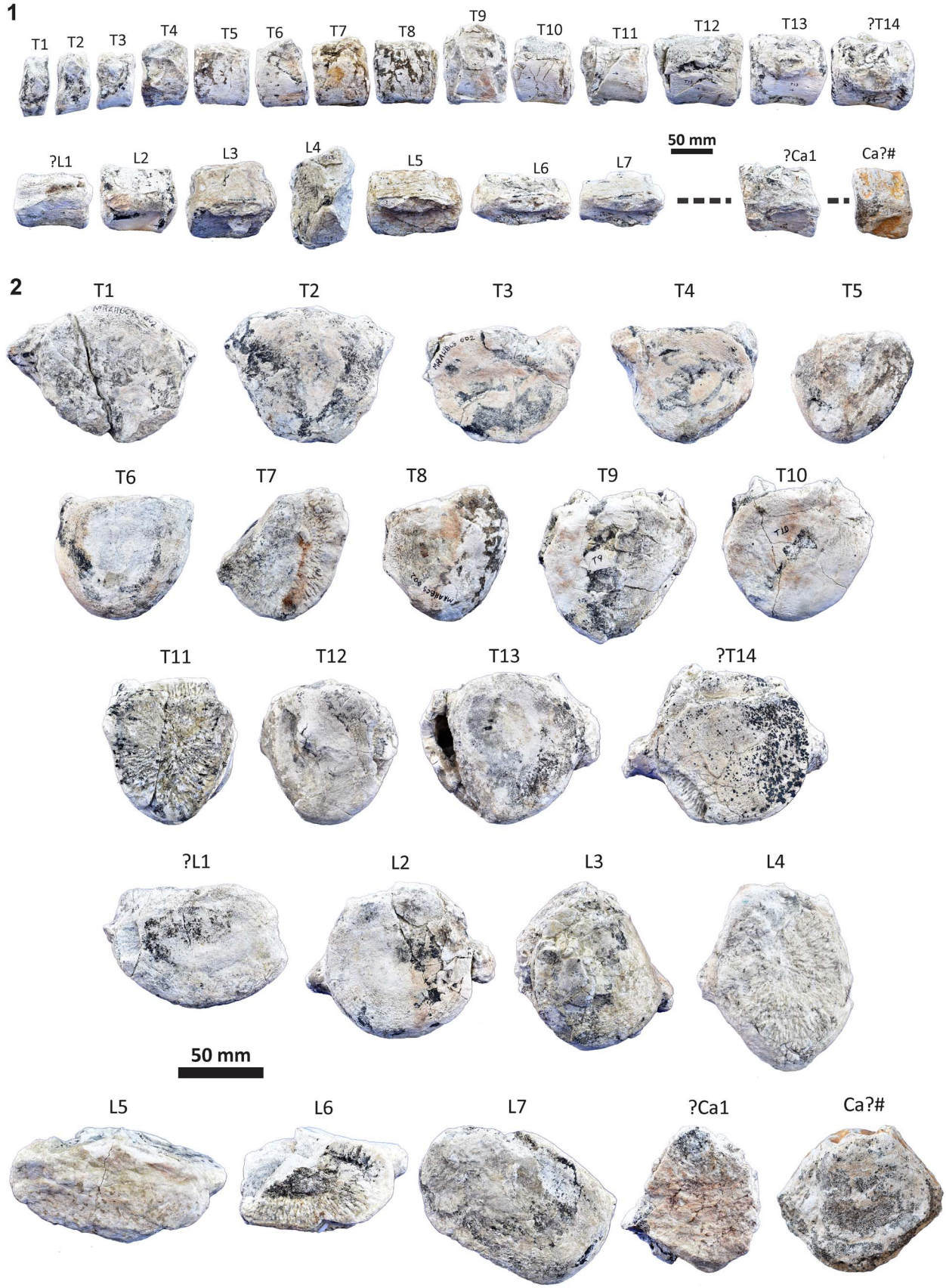

Figure 15. *Echericetus novellus* n. gen. n. sp., holotype, MRAHBCS Pal/V119. (**1, 2**) Thoracic, lumbar, and caudal vertebrae series: (**1**) lateral views; (**2**) anterior views.

https://doi.org/10.1017/jpa.2023.80 Published online by Cambridge University Press

whales (e.g., Clementz et al., 2014; Boessenecker and Fordyce, 2015b), eomysticetids were likely outcompeted by more derived modern-looking mysticetes (early balaenopterids and balaenids; see Tsai, 2023 for early crown mysticetes), with efficient strategies for filter feeding. Notably, the ontogeny of *Waharoa ruwhenua* Boessenecker and Fordyce, 2015b shows the peramorphic process of acceleration, an archaic equivalent to balaenopterids (Tsai and Fordyce, 2014). If the interpretation of this developmental factor is correct, eomysticetids should have represented a relatively diverse and high-disparity clade, similar to modern balaenopterids, making them less vulnerable to extinction. Following this argument, an alternative hypothesis that has yet to be considered is that eomysticetids did not go extinct per se but evolved into a modern-looking baleen whale lineage, analogous to archaeocete–neocete (e.g., de Muizon et al., 2019) or dinosaur–bird transition (e.g., Brusatte et al., 2014). Developmental processes often reveal unexpected deep homology. If our hypothesis turns out to be correct, eomysticetids may have been early crown mysticetes (also see Tsai, 2023 for the origin of crown Mysticeti). Future finds with more complete specimens, accurate geochronological correlation, disparity analyses, detailed examination of morphological characters (similar to new character identification and combination revealing the pygmy right whale to be a cetotheriid; Fordyce and Marx, 2013), and ancestor–descendant tests (see Tsai and Fordyce, 2015a for using ontogenetic clades to bracket the ancestral species) should uncover the hidden baleen whale transitions.

How did Eomysticetidae rise, and what biological and physical factors led to their diversification? In contrast to the toothed mysticetes (e.g., aetiocetids), these questions are crucial to understanding the bloom and evolution of baleen whales because eomysticetids likely represent the first fully baleen-assisted lineage (with nonfunctional teeth; Boessenecker and Fordyce, 2015a). Eomysticetids were probably driven by food sources (e.g., zooplankton; Clementz et al., 2014; Marx et al., 2019; Hernández-Cisneros and Nava-Sánchez, 2022) that seem related to phosphogenetic episodes during the Oligocene (Bisconti et al., 2023). Still, the relationship between the physical conditions and marine ecological systems that have facilitated eomysticetid diversification remains uncertain. Physical factors (e.g., origins and effects of the Antarctic Circumpolar Current) have been proposed as the critical drivers of the neocete evolution (e.g., Fordyce, 1977, 2003; Steeman et al., 2009). However, the impact of the Antarctic Circumpolar Current has been questioned due to the uncertain geochronologic timings, disparate phylogenetic interpretations, and lack of ecological approaches, resulting in the poor explanation of the Oligocene cetacean diversity (Rabosky, 2014; Marx et al., 2016; Pyenson, 2017). By contrast, an integrative approach is growing to explain cetacean evolution regarding global factors such as specific geological events (e.g., massive phosphorite deposition; Bisconti et al., 2023). Further and detailed biogeographic modelings with more eomysticetids discoveries may help to facilitate paleobiological interpretations and which ancestry lineage evolved into eomysticetids at the Eocene–Oligocene boundary. Given the eomysticetid global distribution in the Oligocene, they may have displayed high dispersal ability, leading to the colonization of new geographic areas and diversification. Alternatively, the dispersal events may imply long-distance migratory behavior (Clementz et al., 2014; Boessenecker and Fordyce, 2015b) or indicate intense competition driving niche partitioning (Tsai and Ando, 2015) and dispersal.

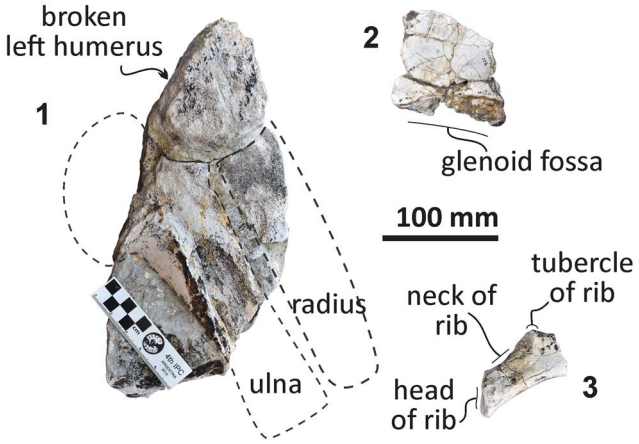

Figure 16. *Echericetus novellus* n. gen. n. sp., holotype, MRAHBCS PAL/V118. (**1**) Left humerus, ulna, and radius in medial view. (**2**) Fragment of right scapula, lateral view. (**3**) Fragment of the right fifth or six rib.

Last, a comprehensive paleobiogeographic framework for the Eomysticetidae remains immature to answer the origin, subsequent dispersal, and speciation events. The richness of eomysticetid occurs primarily in the Southern Hemisphere (New Zealand; Boessenecker and Fordyce, 2017b), which could indicate that eomysticetids originated in the Southern Hemisphere, but contrast with the oldest record of eomysticetids in the North Hemisphere. Given the synapomorphies and phylogenetic positions of *Sitsqwayk* and *Maiabalaena* within eomysticetids (Fig. 17; also see Boessenecker et al., 2023), *Sitsqwayk* and *Maiabalaena* likely represent highly disparate and early- or late-diverging eomysticetids that inhabited the North Pacific. Such a scenario and taxonomic composition indicate a critical differentiation between the south and north cetacean faunas in the Pacific Ocean, indicating the potential of finding more archaic chaeomysticetes from the North Pacific than from the South Pacific. This pattern may suggest a translocating event from the Northern Hemisphere to the colonization of southern oceans by archaic eomysticetids.

Acknowledgments

We thank the Museo Regional de Antropología e Historia de Baja California Sur for granting access to MRAHBCS Pal/V119 (*Echericetus novellus*, dubbed as Mazapán); to J.A. Zuñiga de la Toba and Q. Muñoz Garayzar for access to the collection and support during the preparation of MRAHBCS Pal/V119; and to A. Calderon Vega for allowing us to continue this work. We thank A. Piñeda Geraldo, A. Rosales López, G. González Barba, and collaborators for collecting MRAHBCS Pal/V119 in 1995. We also thank the handling editor, C. Scott, and two anonymous reviewers for constructive suggestions. We are grateful to locals from Rancho La Palma for their help during field visits and to everyone who helped in various ways during this study. A.E.H.-C. was a PhD student at the Instituto

https://doi.org/10.1017/jpa.2023.80 Published online by Cambridge University Press

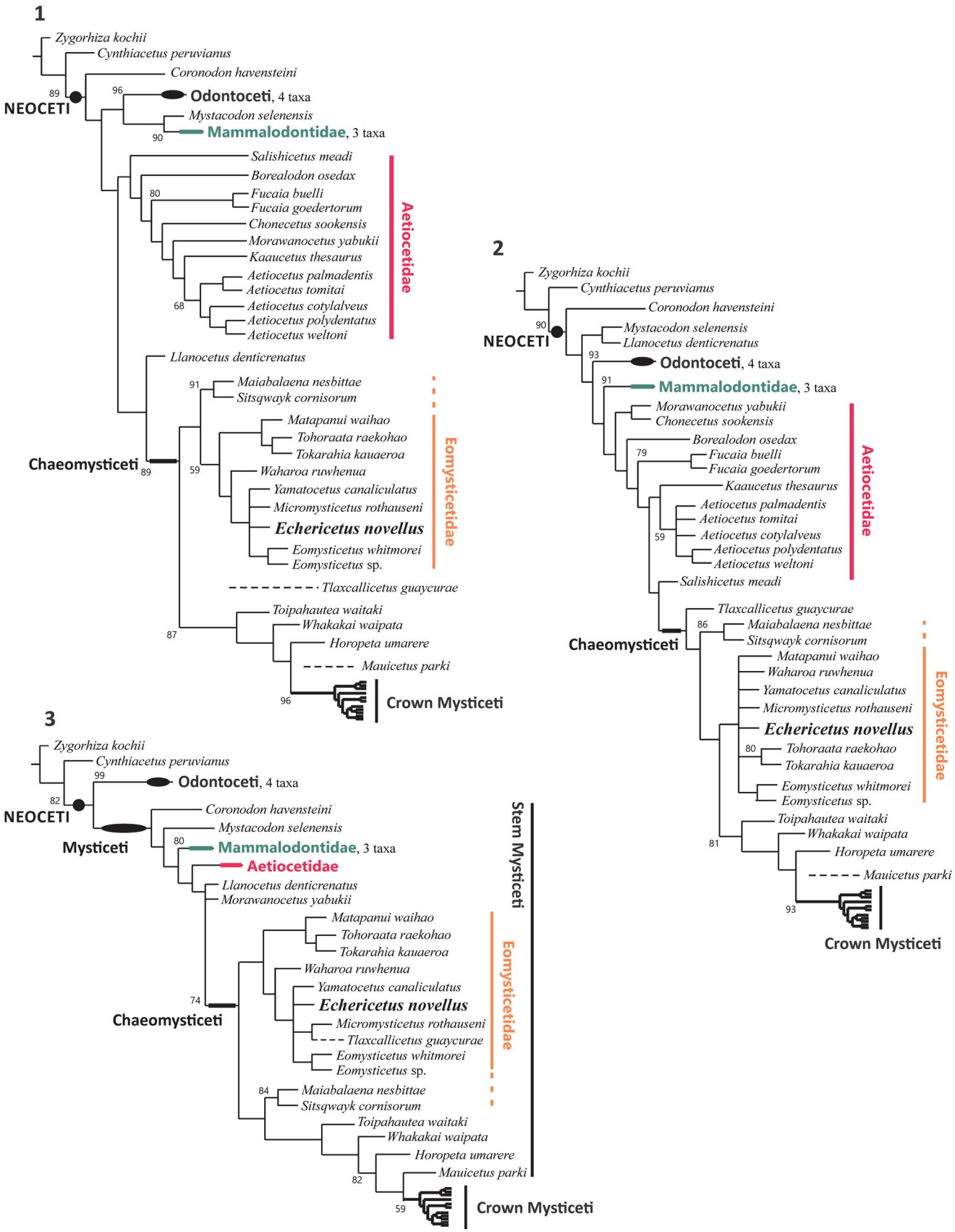

Figure 17. Phylogenetic position of *Echericetus novellus* n. gen. n. sp. under implied weights and equal weights. (**1**) Consensus tree from nine parsimonious trees: k = 28.18360; 30.77813 steps; CI = 0.254; RI = 0.752; RCI = 0.191008; tree total length 1,424. (**2**) Consensus tree from 20,160 parsimonious trees: equal weights; 1,434 steps; CI= 0.242; RI= 0.736; RCI = 0.178112; tree total length 1,494. (**3**) Consensus tree from nine parsimonious trees: k = 3; 129.26216 steps; CI = 0.248; RI = 0.743; RCI = 0.184264; tree total length 1462. Only the support branch > 50% is illustrated.

https://doi.org/10.1017/jpa.2023.80 Published online by Cambridge University Press

Politécnico Nacional - Centro Interdisciplinario de Ciencias Marinas (CICIMAR-IPN), supported by the Consejo Nacional de Ciencia y Tecnología (CONACYT), scholarship 290143 (2017–2021). C.-H.T. was financially supported by the Taiwan Ministry of Science and Technology (now known as National Science and Technology Council; MOST 108-2621-B-002-006-MY3; 111-2621-B-002-006; 112-2621-B-002-005) and public donations to the Lab of Evolution and Diversity of Fossil Vertebrates at the National Taiwan University (NTU FD107028) led by C.-H.T. A.E.H.-C. is grateful to M.R. Cisneros Renteria, F. Hernández Valencia, and the family for their support and care during convalescence, making it possible to finish the present work.

Declaration of competing interests

The authors declare no competing interests.

Data availability statement

Data available from the Dryad Digital Repository: https://doi.org/10.5061/dryad.70rxwdc4s

References

Alvarado-Gastelum, R., 2007, *Estratigrafía de capas rojas y unidades adyacentes en el área de Punta Coyote, Baja California Sur, México* [B.Sc. thesis]: La Paz, Universidad Autónoma de Baja California Sur, 86 p.

Aranda-Gómez, J.J., and Pérez-Venzor, J.A., 1988, Estudio geológico de Punta Coyotes, Baja California Sur: Revista Mexicana de Ciencias Geológicas, v. 7, p. 1–21.

Barnes, L.G., 1998, The sequence of fossil marine mammal assemblages in Mexico: Avances en Investigación, Paleontología de Vertebrados, Publicación Especial, v. 1, p. 26–79.

Benham, W.B., 1937, Fossil Cetacea of New Zealand II.- On *Lophocephalus*, a new genus of zeuglodont Cetacea: Transactions Royal Society of New Zealand v. 67, p. 1–7.

Bisconti, M., Pellegrino, L., and Carnevale, G., 2023, The chronology of mysticete diversification (Mammalia, Cetacea, Mysticeti): body size, morphological evolution and global change: Earth-Science Reviews, v. 239, n. 104373, https://doi.org/10.1016/j.earscirev.2023.104373.

Boessenecker, R.W., 2022, Oligocene–Miocene marine mammals from Belgrade Quarry, North Carolina: Geobios, v. 74, p. 1–19.

Boessenecker, R.W., and Fordyce, R.E., 2015a, A new genus and species of eomysticetid (Cetacea: Mysticeti) and a reinterpretation of "*Mauicetus*" *lophocephalus* Marples, 1956: transitional baleen whales from the upper Oligocene of New Zealand: Zoological Journal of the Linnean Society, v. 175, p. 607–660.

Boessenecker, R.W., and Fordyce, R.E., 2015b, Anatomy, feeding ecology, and ontogeny of a transitional baleen whale: a new genus and species of Eomysticetidae (Mammalia: Cetacea) from the Oligocene of New Zealand: PeerJ, v. 3, n. e1129, https://doi.org/10.7717/peerj.1129.

Boessenecker, R.W., and Fordyce, R.E., 2017a, A new eomysticetid from the Oligocene Kokoamu Greensand of New Zealand and a review of the Eomysticetidae (Mammalia, Cetacea): Journal of Systematic Palaeontology, v. 15, p. 429–469.

Boessenecker, R.W., and Fordyce, R.E., 2017b, Cosmopolitanism and Miocene survival of Eomysticetidae (Cetacea: Mysticeti) revealed by new fossils from New Zealand: New Zealand Journal of Geology and Geophysics, v. 60, p. 145–157.

Boessenecker, R.W., Beatty, B.L., and Geisler, J.H., 2023, New specimens and species of the Oligocene toothed baleen whale *Coronodon* from South Carolina and the origin of Neoceti: PeerJ, v. 11, n. e14795, https://doi.org/10.7717/peerj.14795.

Brisson, M.J., 1762, Regnum Animale in Classes IX Distributum, Sive Synopsis Methodica Sistens Generalem Animalium Distributionem in Classes IX, et Duarum Primarum Classium, Quadrupedum Scilicet and Cetaceorum, Particulare Divisionem in Ordines, Sectiones, Genera, et Species: Paris, T. Haak, 296 p.

Brusatte, S.L., Lloyd, G.T., Wang, S.C., and Norell, M.A., 2014, Gradual assembly of avian body plan culminated in rapid rates of evolution across the dinosaur–bird transition: Current Biology, v. 24, p. 2386–2392.

Clementz, M.T., Fordyce, R.E., Peek, S.L., and Fox, D.L., 2014, Ancient marine isoscapes and isotopic evidence of bulk-feeding by Oligocene cetaceans: Palaeogeography Palaeoclimatology, Palaeoecology, v. 400, p. 28–40.

Cohen, K.M., Harper, D.A.T., and Gibbard, P.L., 2023, ICS International Chronostratigraphic Chart 2023/09: International Commission on Stratigraphy, IUGS, www.stratigraphy.org/chart.

Corrie, J.E., and Fordyce, R.E., 2022, A redescription and re-evaluation of *Kekenodon onamata* (Mammalia: Cetacea), a late-surviving archaeocete from the late Oligocene of New Zealand: Zoological Journal of the Linnean Society, v. 196, p. 1637–1670.

de Muizon, C., Bianucci, G., Martínez-Cáceres, M., and Lambert, O., 2019, *Mystacodon selenensis*, the earliest known toothed mysticete (Cetacea, Mammalia) from the late Eocene of Peru: anatomy, phylogeny, and feeding adaptations: Geodiversitas, v. 41, p. 401–499.

Drake, W.R., Umhoefer, P.J., Griffiths, A., Vlad, A., Peters, L., and McIntosh, W., 2017, Tectono-stratigraphic evolution of the Comondú Group from Bahía de La Paz to Loreto, Baja California Sur, Mexico: Tectonophysics, v. 719–720, p. 107–115, 123–134.

Ekdale, E.G., and Deméré, T.A., 2022, Neurovascular evidence for a co-occurrence of teeth and baleen in an Oligocene mysticete and the transition to filter-feeding in baleen whales: Zoological Journal of the Linnean Society, v. 194, p. 395–415.

Fischer, R., Galli-Ollivier, C., Gidde, A., and Schwennicke, T., 1995, The El Cien Formation of southern Baja California, Mexico: stratigraphic precisions: Newsletters in Stratigraphy, v. 32, p. 137–161.

Fordyce, R.E., 1977, The development of the Circum-Antarctic Current and the evolution of the Mysticeti (Mammalia: Cetacea): Palaeogeography Palaeoclimatology, Palaeoecology, v. 21, p. 265–271.

Fordyce, R.E., 2003, Cetacean evolution and Eocene–Oligocene oceans revisited, in Prothero, D.R., Ivany, L.C., and Nesbitt, E., eds., From Greenhouse to Icehouse: New York, Columbia University Press, p. 154–170.

Fordyce, R.E., and Marx, F.G., 2013, The pygmy right whale *Caperea marginata*: the last of the cetotheres: Proceedings of the Royal Society B, v. 280, 20122645, https://doi.org/10.1098/rspb.2012.2645.

Fordyce, R.E., and Marx, F.G., 2018, Gigantism precedes filter feeding in baleen whale evolution: Current Biology, v. 28, p. 1670–1676.

Gatesy, J., Ekdale, E.G., Deméré, T.A., Lanzetti, A., Randall, J., Berta, A., El Adli, J.J., Springer, M.S., and McGowen, M.R., 2022, Anatomical, ontogenetic, and genomic homologies guide reconstructions of the teeth-to-baleen transition in mysticete whales: Journal of Mammalian Evolution, v. 29, p. 891–930.

Goloboff, P.A., 1993, Estimating character weights during tree search: Cladistics, v. 9, p. 83–91.

Goloboff, P.A., and Catalano, S.A., 2016, TNT version 1.5, including a full implementation of phylogenetic morphometrics: Cladistics, v. 32, p. 221–238.

Goloboff, P.A., Farris, J.S., Källersjö, M., Oxelman, B., and Szumik, C.A., 2003, Improvements to resampling measures of group support: Cladistics, v. 19, p. 324–332.

Goloboff, P.A., Carpenter, J.M., Arias, J.S., and Miranda-Esquivel, D.R., 2008, Weighting against homoplasy improves phylogenetic analysis of morphological data sets: Cladistics, v. 24, p. 758–773.

Goloboff, P.A., Torres, A., and Arias, J.S., 2018, Weighted parsimony outperforms other methods of phylogenetic inference under models appropriate for morphology: Cladistics, v. 34, p. 407–437.

Gray, J.E., 1864, On the cetaceous mammals, in Richardson, J., and Gray, J.E., eds., The Zoology of the Voyage of the H.M.S. Erebus and Terror, under the Command of Captain Sir JC Ross, RN, FRS, during the Years 1839 to 1843, Volumes 1 and 2: London, E.W. Janson, p. 1–53.

Hausback, B.P., 1984, Cenozoic volcanic and tectonic evolution of Baja California Sur, Mexico, in Frizzel, V.A., Jr., ed., Geology of the Baja California Peninsula: Pacific Section, Society of Economic Paleontologists and Mineralogists, p. 219–236.

Hernández-Cisneros, A.E., 2018, A new group of late Oligocene mysticetes from Mexico: Palaeontologia Electronica, v. 21, n. 21.1.7A, http://dx.doi.org/10.26879/746.

Hernández-Cisneros, A.E., 2022, A new aetiocetid (Cetacea, Mysticeti, Aetiocetidae) from the late Oligocene of Mexico: Journal of Systematic Palaeontology, v. 20, https://doi.org/10.1080/14772019.2022.2100725.

Hernández-Cisneros, A.E., and Nava-Sánchez, E.H., 2022, Oligocene dawn baleen whales in Mexico (Cetacea, Eomysticetidae) and palaeobiogeographic notes: Paleontología Mexicana, v. 11, p. 1–12.

INEGI, 2007, Carta topográfica La Paz G12-10-11: Instituto Nacional de Estadística Geográfica e Informática, scale 1:250 000, 1 sheet.

INEGI, 2017, Carta topográfica San José del Cabo F1202030506: Instituto Nacional de Estadística Geográfica e Informática, scale 1:250 000, 1 sheet.
Martínez-Cáceres, M., Lambert, O., and de Muizon, C., 2017, The anatomy and phylogenetic affinities of *Cynthiacetus peruvianus*, a large Dorudon-like basilosaurid (Cetacea, Mammalia) from the late Eocene of Peru: Geodiversitas, v. 39, p. 7–163.
Marx, F.G., and Fordyce, R.E., 2015, Baleen boom and bust: a synthesis of mysticete phylogeny, diversity, and disparity: Royal Society Open Science, v. 2, n. 140434, https://doi.org/10.1098/rsos.140434.
Marx, F.G., Lambert, O., and Uhen, M.D., 2016, Cetacean Paleobiology: West Sussex, Wiley-Blackwell, 319 p.
Marx, F.G., Collareta, A., Gioncada, A., Post, A., Lambert, O., Bonaccorsi, E., Urbina, M., and Bianucci, G., 2017, How whales used to filter: exceptionally preserved baleen in a Miocene cetotheriid: Journal of Anatomy, v. 231, p. 212–220.
Marx, F.G., Fitzgerald, E.M.G., and Fordyce, R.E., 2019, Like phoenix from the ashes: how modern baleen whales arose from a fossil "dark age": Acta Palaeontologica Polonica, v. 64, p. 231–238.
McFall, C.C., 1968, Reconnaissance geology of the Concepción Bay area, Baja California Sur, Mexico: Stanford University Publications in Geological Science, v. 10, 25 p.
Mead, J.G., and Fordyce, R.E., 2009, The therian skull: a lexicon with emphasis on the odontocetes: Smithsonian Institution Scholarly Press, https://doi.org/10.5479/si.00810282.627.
Okazaki, Y., 2012, A new mysticete from the upper Oligocene Ashiya Group, Kyushu, Japan and its significance to mysticete evolution: Bulletin of the Kitakyushu Museum of Natural History and Human History, Series A, v. 10, p. 129–152.
Peredo, C.M., and Pyenson, N.D., 2018, *Salishicetus meadi*, a new aetiocetid from the late Oligocene of Washington State and implications for feeding transitions in early mysticete evolution: Royal Society Open Science, v. 5, n. 172336, http://dx.doi.org/10.1098/rsos.172336.
Peredo, M.C., and Uhen, M.D., 2016, A new basal chaeomysticete (Mammalia: Cetacea) from the late Oligocene Pysht Formation of Washington, USA: Papers in Palaeontology, v. 2, p. 533–554, https://doi.org/10.1002/spp2.1051.
Peredo, C.M., Pyenson, N.D., Marshall, C.D., and Uhen, M.D., 2018, Tooth loss precedes the origin of baleen in whales: Current Biology, v. 28, p. 3992–4000.
Plata-Hernández, E., 2002. Cartografía y estratigrafía del área de Timbabichi, Baja California Sur, México [B.Sc. thesis]: La Paz, Universidad Autónoma de Baja California Sur, 113 p.
Pyenson, N.D., 2017, The ecological rise of whales chronicled by the fossil record: Current Biology, v. 27, p. R558–R564.
Rabosky, D.L., 2014, Automatic detection of key innovations, rate shifts, and diversity-dependence on phylogenetic trees: PLoS ONE, v. 9, n. e89543, http://dx.doi.org/10.1371/journal.pone.0089543.
Sanders, A.E., and Barnes, L.G., 2002a, Paleontology of the late Oligocene Ashley and Chandler Bridge Formations of South Carolina, 2: *Micromysticetus rothauseni*, a primitive cetotheriid mysticete (Mammalia: Cetacea): Smithsonian Contributions to Paleobiology, v. 93, p. 271–293.
Sanders, A.E., and Barnes, L.G., 2002b, Paleontology of the late Oligocene Ashley and Chandler Bridge Formations of South Carolina, 3: Eomysticetidae, a new family of primitive mysticetes (Mammalia: Cetacea): Smithsonian Contributions to Paleobiology, v. 93, p. 313–356.
Schipps, B.K., Peredo, C.M., and Pyenson, D., 2019, *Borealodon osedax*, a new stem mysticete (Mammalia, Cetacea) from the Oligocene of Washington State and its implications for fossil whale-fall communities: Royal Society Open Science, v. 6, n. 182168, https://doi.org/10.1098/rsos.182168.
Schöllhorn, I., Houben, A., Gertsch, B., Adatte, T., Alexey, U., de Kaenel, E., Spangenberg, J.E., Janssen, N., Schwennicke, T., and Föllmi, K.B., 2020, Enhanced upwelling and phosphorite formation in the northeastern Pacific during the late Oligocene: depositional mechanisms, environmental conditions, and the impact of glacio-eustacy: Geological Society of America Bulletin, v. 132, p. 687–709, https://doi.org/10.1130/B32061.1.
Schwennicke, T., González-Barba, G., and de Anda-Franco, N., 1996, Lower Miocene marine and fluvial beds at Rancho La Palma, Baja California Sur, Mexico: Boletín del Departamento de Geología de la Universidad de Sonora, v. 13, no. 1, p. 1–14.
Schwennicke, T., Plata-Hernández, E., and Vázquez-Balderas, J.F., 2000, Stratigraphy of Oligocene–Miocene Red Beds in central Baja California Sur, México: XVII Simposio sobre la Geología de Latinoamérica, Stutgart, Germany, extended abstracts, v. 18, p. 1–6.
Schwennicke, T., Alvarado Gastelum, R., and Pérez-Venzor, J.A., 2006, La Formación Salto en el valle Coyote, Baja California Sur: Implicaciones estratigráficas y regionales: V Reunión Nacional de Ciencias de la Tierra, Puebla, México, Abstracts, v. 5, p. 20–21.
Steeman, M.E., Hebsgaard, M.B., Fordyce, R.E., Ho, S.Y.W., Rabosky, D.L., Nielsen, R., Rahbek, C., Glenner, H., Sørensen, M.V., and Willerslev, E., 2009, Radiation of extant cetaceans driven by restructuring of the oceans: Systematic Biology, v. 58, p. 573–585.
Tsai, C.-H., 2023, In search of the origin of crown Mysticeti: Journal of the Royal Society of New Zealand, https://doi.org/10.1080/03036758.2023.2249410.
Tsai, C.-H., and Ando, T., 2015, Niche partitioning in Oligocene toothed mysticetes (Mysticeti: Aetiocetidae): Journal of Mammalian Evolution, v. 23, p. 33–41.
Tsai, C.-H., and Fordyce, R.E., 2014, Juvenile morphology in baleen whale phylogeny: Naturwissenschaften, v. 101, p. 765–769, https://doi.org/10.1007/s00114-014-1216-9.
Tsai, C.-H., and Fordyce, R.E., 2015a, Ancestor–descendant relationships in evolution: origin of the extant pygmy right whale, *Caperea marginata*: Biology Letters, v. 11, n. 20140875, https://doi.org/10.1098/rsbl.2014.0875.
Tsai, C.-H., and Fordyce, R.E., 2015b, The earliest gulp-feeding mysticete (Cetacea: Mysticeti) from the Oligocene of New Zealand: Journal of Mammalian Evolution, v. 22, p. 535–560, https://doi.org/10.1007/s10914-015-9290-0.
Tsai, C.-H., and Fordyce, R.E., 2016, Archaic baleen whale from the Kokoamu Greensand: earbones distinguish a new late Oligocene mysticete (Cetacea: Mysticeti) from New Zealand: Journal of the Royal Society of New Zealand, v. 46, p. 117–138. https://doi.org/10.1080/03036758.2016.1156552.
Tsai, C.-H., and Fordyce, R.E., 2018, A new archaic baleen whale *Toipahautea waitaki* (early late Oligocene, New Zealand) and the origins of crown Mysticeti: Royal Society Open Science, v. 5, n. 172453, http://dx.doi.org/10.1098/rsos.172453.
Tsai, C-H., and Kohno, N., 2016, Multiple origins of gigantism in stem baleen whales: The Science of Nature, v. 103, n. 89, https://doi.org/10.1007/s00114-016-1417-5.
Umhoefer, P.J., Dorsey, R.J. Willsey, S., Mayer, L., and Renne, P., 2001, Stratigraphy and geochronology of the Comondu Group near Loreto, Baja California Sur, Mexico, in Halfar, J., and Nava-Sánchez, E.H., eds., Sedimentation and Tectonics of an Active Rift Basin Margin: The Gulf of California: Sedimentary Geology, Special issue, v. 144, p. 125–147.
Walsh, B.M., and Berta, A., 2011, Occipital ossification of balaenopteroid mysticetes: Anatomical Record, v. 294, p. 391–398.
Watson, A.G., and Fordyce, R.E., 1993, Skeleton of two minke whales, *Balaenoptera acutorostrata*, stranded on the southeast coast of New Zealand: New Zealand Natural Sciences, v. 20, p. 1–14.

Accepted: 4 October 2023